Theory of light scattering by the spin-wave excitations of thin ferromagnetic films

R. E. Camley
Max Planck Institut für Festkörperforschung, 1 Heisenbergstrasse, Stuttgart, West Germany

Talat S. Rahman and D. L. Mills
Department of Physics, University of California, Irvine, California 92717
(Received 7 July 1980; revised manuscript received 2 September 1980)

We discuss the theory of light scattering by surface and standing spin-wave excitations of a thin ferromagnetic film with magnetization parallel to the surface. The theory includes the influence of both exchange and dipolar interactions between the spins, the effect of the demagnetizing field generated by the spin motion, and spin pinning at both the upper and lower surface. We use the theory to carry out a series of numerical studies of the light scattering spectra which illustrate a number of general features of the scattering process. We compare the results of the calculations with the recent experimental data of Grimsditch, Malozemoff, and Brunseh.

I. INTRODUCTION

The study of the frequencies of standing spin waves in thin films has given us insight on the exchange constants of ferromagnetic materials, the renormalization of spin-wave frequencies by magnon-magnon interactions, and other intrinsic properties of spin-wave excitations in magnetic crystals. It can also provide information about the influence of a surface or an interface on the spin motion, since spins located in its vicinity may have their motion inhibited by "pinning" fields of either extrinsic or intrinsic origin.

Until recently microwave resonance studies have provided all of the data available on standing spin waves in thin films.[1] In these experiments, a sample is placed in a cavity with a particular resonance frequency, and the various spin-wave modes are swept through the cavity resonance by varying an external magnetic field.

Recently standing spin waves in thin films,[2] and also spin waves near the surface of thick samples[3] have been probed in light scattering experiments. In these measurements, a laser photon with frequency ω_0, and vacuum wave vector $\vec{k}^{(0)}$ is directed onto the material to scatter off of a spin wave inelastically, with a shifted frequency $\omega_s = \omega_0 \pm \Omega$, where Ω is the frequency of the spin wave absorbed or created in the scattering process. One measures the frequency spectrum of the scattered light, for a fixed value of the Zeeman field. In the experiments of interest to the present paper, the incident light is absorbed strongly by the substrate, and the skin depth δ is roughly 200 Å. Under these conditions, where the optical skin depth is small compared to the wavelength of light in the vacuum, components of the wave vector normal to the surface are not conserved in the scattering process.[4] Wave-vector components parallel to the surface are conserved, however, so we have $\vec{k}_{\parallel}^{(s)} = \vec{k}_{\parallel}^{(0)} \pm \vec{Q}_{\parallel}$, where the subscript denotes the projection of a given wave vector onto the plane parallel to the surface, $\vec{Q}$ and $\vec{k}^{(s)}$ being the wave vectors of the spin wave and the scattered photon, respectively.

The spin-wave frequency Ω is very small compared to either ω_0 or ω_s. Under these conditions, all spin-wave excitations (surface modes, bulk modes) characterized by the same value of $\vec{Q}_{\parallel}$ scatter the incident light in the same final direction. Thus, the light scattering measurement produces, for a single value of the Zeeman field, information on a large number of spin-wave excitations whose frequency and, in principle, the linewidth can be followed as a continuous function of the magnetic field. The method thus provides far more insight than that obtained from resonance measurements, though with present day Fabry-Perot spectrometers the microwave cavity method offers far superior resolution.

This paper presents the theory of light scattering from spin-wave excitations in thin films, within the framework of a treatment that includes both dipolar and exchange interactions in the spin system. We have carried out a series of numerical studies of scattering from standing and surface spin waves in the film geometry, with the aim of elucidating the nature of the coupling between the light and the spin waves, and the factors that control the relative intensities of the spin-wave features in the Brillouin spec-

trum.[5,6] The analysis here can be regarded as an extension of the earlier work of Camley and Mills,[7] who explored the scattering of light by bulk and surface spin waves in a semi-infinite geometry. The calculations presented here are the result of a more complete consideration of the influence of the scattering geometry on the light than that carried out earlier. Consequently, we have also included some characteristic of the phenomena present in the semi-infinite case. We should note that Cottam has also discussed light scattering from spin waves in films.[8] However, his theory does not include exchange interactions between spins and the possible effect of spin pinning on the light scattering. The former plays a crucial role in the light scattering spectra of all the materials which have so far been examined experimentally, except for the europium chalcogenides,[7] while the latter is suggested to be important in some materials.[2] Before we turn to detailed discussions, some introductory remarks which compare the light scattering and resonance methods may prove useful.

In microwave resonance studies, the film is illuminated by radiation with wavelength of the order of 1 cm. This is typically large compared to both the film thickness and the width of the film. For metallic films, such as we consider here, an important parameter is the ratio of the skin depth δ to the film thickness L. At microwave frequencies, in a material such as iron, the skin depth is the order of 1 μm; so $\delta >> L$ for film thicknesses in the range of a few hundred angstroms. The microwave field is thus spatially uniform within the film, to an excellent approximation. In this situation, spin pinning influences the mode intensities in a crucial way, as has been well known for many years.[9] We illustrate this in Fig. 1 where, for the case where dipole interactions are ignored and only exchange coupling between the spins is present, we sketch the distribution of transverse magnetization $m_+(y)$ when spin-wave modes are excited. In the limit of no pinning, the boundary condition reads[9] $[\partial m_+(y)/\partial y]=0$ at both surfaces. The lowest mode has wave-vector components normal to the surface, $k_\perp^{(0)}$, equal to zero. This uniform mode, labeled $n=0$ in Fig. 1(a), absorbs microwaves strongly, since all spins precess coherently and with the same phase. The higher modes have $k_\perp^{(n)}=n\pi/L$, as shown in the sketch. In the absence of pinning and when $\delta >> L$, only the uniform mode is observed experimentally since, as one can see from the sketch, $\int_0^L dy\, m_+^{(n)}(y)$ vanishes for all other modes. The integral measures the total transverse magnetic moment associated with the spin wave, and it is this quantity that couples to the spatially uniform microwave field. In the opposite limit of very strong pinning, the condition that m_+ is to vanish at the boundaries leads to the mode structure illustrated in Fig. 1(b). The lowest mode has $k_\perp^{(1)}=\pi/L$, and absorbs strongly. In fact, all modes with $k_\perp^{(n)}=n\pi/L$, where n is an odd integer will absorb microwave radiation, while those with n even will not since $\int_0^L dy\, m_+^{(n)}(y)$ vanishes for them.

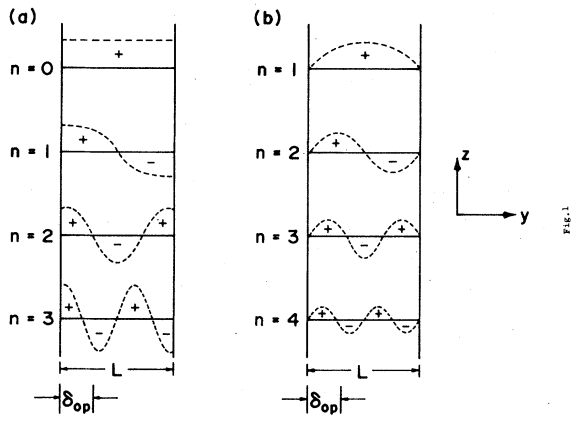

FIG. 1. Sketch of the transverse magnetization $m_+^{(n)}(y)$ associated with the standing spin-wave resonances of a thin film in (a) the limit of zero pinning and (b) the limit of strong pinning.

The above discussion shows that in microwave resonance, pinning influences the mode intensities in a crucial way, and in fact in a uniform film pinning is necessary for the study of the spin-wave spectrum of the sample and one has to rely on the presence of an extrinsic mechanism to render the modes visible.[10] In practice, one is rarely in the strong pinning limit illustrated in Fig. 1(b), but rather in a regime where the spin motion in the surface is only partially inhibited by the local effective fields. Then the allowed standing-wave resonances have wave vectors perpendicular to the surface given by $k_\perp^{(n)}=(n\pi+\delta_n)/L$, with $n=0, 1, 2, \ldots$, and δ_n is a phase shift that lies between 0 and π. We have $\delta_n=0$ with no pinning, $\delta_n=\pi$ in the limit of very strong pinning, and in the intermediate regime one must understand the nature of the pinning fields to know the values assumed by $k_\perp^{(n)}$; ultimately this leads to uncertainty in the determination of the exchange stiffness constant D by microwave resonance methods, since the frequency splitting between adjacent standing-wave resonances of the film is controlled by the quantity $D[k_\perp^{(n+1)2}-k_\perp^{(n)2}]$.

In the light scattering experiments, the driving field has a qualitatively different spatial dependence, and this affects the influence of pinning on the mode intensities in a fundamental fashion. The electromagnetic fields in the scattering experiments are nonzero only within the optical skin depth, which is roughly 200 Å for the ferromagnetic metals and alloys. For typical films, we are now in the limit $\delta << L$, where δ is the penetration depth of the exciting fields. For the films used by Grimsditch *et al.*,[2] we have

$\delta_{op}/L \cong 0.25$, as illustrated schematically in Fig. 1. The matrix element for exciting a spin wave now assumes the form $\int_0^\infty dy\, m_+(y) \exp(-2y/\delta)$, where the factor of 2 enters because the nonlinear term in the Hamiltonian which couples the light to the spin motion involves the product of the incident and the scattered electromagnetic fields.[11] It is quite clear that when $\delta/L << 1$, even in the limit of zero pinning, *all* of the standing spin-wave resonances of the film can be excited in light scattering measurements. Thus, for well-prepared films with small intrinsic pinning fields, it should be possible, in principle, to obtain accurate values of D from the mode separations in the light scattering method, under circumstances where the allowed spin-wave frequencies may be accurately computed. It is also clear, as the calculations presented below will illustrate, that for values of δ/L relevant to the experiments of Grimsditch *et al.*,[2] the mode intensities are not affected dramatically by the presence or absence of pinning fields, though as we shall see, the presence of pinning leads to systematic effects in the spectra.

The discussion above contrasts spin-wave excitation by microwave and light scattering methods with attention directed to the spatial variation of the exciting fields in the direction *normal* to the film surface. We now turn to the role of the spatial variation in the exciting fields in the plane of the film surfaces. For the purposes of these remarks, let the film be a square piece of material with sides of length W, and thickness $L << W$.

In microwave experiments, where the radiation is incident normally on the film, the exciting fields are uniform over the surface of the film. Under these circumstances, we expect the wave vector $\vec{Q}_\parallel$ of the spin waves excited in the experiment to be equal to zero. However, in practice, the spins can be strongly pinned at the edges of the film, so with a uniform field one may excite geometrical resonances of the film structure, with $\vec{Q}_\parallel \cong (n\hat{x} + m\hat{y})\pi/W$ where n and m are integers.[12,13] A very beautiful study of modes of this character has been reported by Wigen and coworkers for epitaxially grown yttrium iron garnet films,[14] where they also present a most interesting study of a mode crossing. A detailed discussion of these modes is quite complicated, since the mode positions depend on whether the spins at the film edges are fully or partially pinned.[12]

The light scattering method also excites spin waves with nonzero values of $\vec{Q}_\parallel$. If $\vec{k}_\parallel^{(0)}$ and $\vec{k}_\parallel^{(s)}$ are the wave vectors of the incident and scattered photon projected onto a plane parallel to the film surfaces, we have $\vec{Q}_\parallel = \pm(\vec{k}_\parallel^{(0)} - \vec{k}_\parallel^{(s)})$, with the choice of sign dependent on whether the spin wave is emitted (Stokes process) or absorbed (anti-Stokes process) in the light scattering event. We have $|\vec{Q}_\parallel| \cong 10^5$ cm^{-1} for typical scattering geometries, so the modes excited in light scattering experiments always have $|\vec{Q}_\parallel| W >> 1$. Hence, the film may be regarded as truly infinite in the two directions parallel to the film surfaces, and the spectra are not influenced at all by the presence or absence of pinning at the film edges. Furthermore, as pointed out earlier[7] and as illustrated here, the frequency of the surface modes and the standing-wave resonances is sensitive to the angle between $\vec{Q}_\parallel$ and the saturation magnetization $\vec{M}_s$, which has been assumed to be parallel to the surface. The linewidths can be affected by the magnitude of $\vec{Q}_\parallel$ for fixed direction, and this may be varied over a considerable range by varying the angle of both the incident and scattered radiation relative to the normal to the film surfaces.

The above remarks illustrate that the light scattering method offers a new means of probing spin-wave excitations in thin films, and takes us into a new regime of parameters. It may appear from our discussion that only standing-wave resonances are probed by the method but as seen in the experiments,[7,8] we also find an intriguing set of surface spin-wave modes in the spectra, with intensity comparable to or larger than the bulk spin waves. These surface modes, called the Damon-Eshbach waves, have the curious property that they are unidirectional in character, and on a semi-infinite sample propagate only from left to right across the magnetization, as one views the sample from above. It has been predicted recently[15] that such nonreciprocal surface modes can propagate also on the surface of antiferromagnets. The light scattering method offers a natural means of detecting these modes, which lie in the infrared where absorption spectroscopy is a poor way to detect surface excitations, since the effective absorption volume is very small.

To proceed further with our discussion, we must turn to detailed calculations. In Sec. II, we describe the calculation of the response functions that are central to the discussion, and in Sec. III we briefly outline the details of the light scattering calculation. Then in Sec. IV we present the results of our numerical calculations. We remark that a brief discussion of the same results of the film spectra have been reported elsewhere, with emphasis on the comparison between the calculated spectra, and new measurements.[6]

II. DESCRIPTION OF THERMAL FLUCTUATIONS IN A FERROMAGNETIC FILM

We now discuss the general formalism of the scattering of light from spin waves in thin films. In this section we describe the method of calculating the spectrum of spin fluctuations in the film, and in Sec. III we deal with the coupling of light to the fluctuations. The method we have used is in fact an extension of the earlier work of Ref. 7, which explores

light scattering from spin waves near the surfaces of a semi-infinite sample. Therefore, the discussion here will be brief, though for completeness we present the principal formulas with emphasis on the new features that appear for the finite film.

The geometry of the light scattering experiment is illustrated in Fig. 2. We consider a film with surfaces parallel to the xz plane of a Cartesian coordinate system, so that the y direction is normal to the surface. The magnetization $\vec{M}_s$ is aligned along the z direction, and the film lies in the region $0 \leq y \leq L$. The incident radiation strikes the surface $y = 0$, and the wave vector of the incident photon lies in the xy plane as illustrated. The angles θ_0, θ_s, and ϕ_s measure the direction of the incoming and scattered radiation with respect to the various coordinate axes.

Before we turn to the formalism, it may be useful to comment on the salient features of the method we have used. At low temperatures, where spin-wave theory applies, we could have proceeded like Wolfram and de Wames[1] by analyzing in detail the spin-wave excitations in thin films. Then with the appropriate boson annihilation and creation operators, we could have related the spin-density operators $S_x(\vec{x})$ and $S_y(\vec{x})$ to the normal modes, as Kittel has done.[16] The spin waves could then be coupled to the radiation field and the inelastic light scattering process viewed as an interaction between the quanta of the appropriate quantized fields.

We have chosen to proceed very differently. We calculate certain response functions $\chi_{ij}(\vec{x}\vec{x}';t-t')$ which, through use of identities provided below, may be related to the spectrum of spin fluctuations in the material. These may be found, in the spin-wave regime, without detailed inquiry into the dispersion relation of the individual spin-wave eigenmodes. However, the response functions, when Fourier transformed in the appropriate fashion have poles at the relevant spin-wave frequencies. For a given scattering configuration, like that in Fig. 2, we calculate the frequency spectrum of the scattered light with its various features without explicit reference to the dispersion relations. The response functions, when dissected in the proper fashion, also contain direct information about the eigenvector associated with the mode that produces a particular feature in the light scattering spectrum.

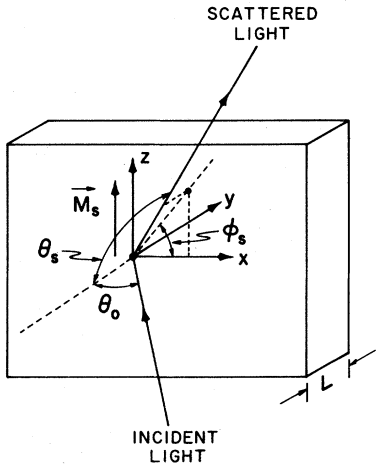

FIG. 2. Scattering geometry of primary interest to the present paper. The incident photon has a wave vector in the xy plane, and for $\phi_s = 0$ the scattered photon has wave vector in the xy plane also. The film has surfaces parallel to the xz plane, and lies in the region $0 \leq y \leq L$, with magnetization parallel to the z direction.

The virtue of this approach is that it leads to closed, relatively simple expressions for the light scattering cross section, though in the present case the algebra is a bit tedious. The inclusion of the damping of the spin motion, within a relaxation time approximation, allows us to study the line shapes as well as the mode intensities.

Finally, the radiation field associated with the incident and scattered laser light is treated by classical methods. This allows us to include fully the effect of the strong absorption of the laser light in the sample, which in the ferromagnetic metals limits the skin depth to roughly 200 Å. This is done by using the observed values of the optical constants of the film for describing electromagnetic fields inside the sample. A theorem in the text by Abrikosov *et al.*[17] ensures that the classical theory produces results identical to those found in the quantum field theory.

The approach to the theory of inelastic light scattering from solids just outlined has been applied to the analysis of a number of different scattering processes, in recent years. We refer the reader elsewhere[4] for a more complete discussion and review of the available literature. We now turn to the details of the method, as it applies to the problem of present interest.

Let $S_i(\vec{x},t)$ be the operator which describes the ith Cartesian component of spin density at point $\vec{x}$ and time t. We then require the form of the correlation functions

$$S_{ij}(\vec{x}\vec{x}';t-t') = \langle S_i(\vec{x},t)S_j(\vec{x}',t')\rangle_0 \ , \qquad (2.1)$$

where $\langle\ \rangle_0$ denotes an average over the appropriate finite-temperature statistical ensemble, in the absence of an external field. In the spin-wave regime, only the correlations with i or j equal to x or y enter.

For a film infinite in both the x and z directions, $S_{ij}(\vec{x}\vec{x}';t-t')$ is a function of only $\vec{x}_{\parallel} - \vec{x}'_{\parallel}$, where $\vec{x}_{\parallel}$ is the projection of $\vec{x}$ onto the xz plane. Hence, we

may write

$$S_{ij}(\vec{x}\vec{x}';t-t') = \int \frac{d^2Q_{\parallel}\,d\Omega}{(2\pi)^3} S_{ij}(yy';\vec{Q}_{\parallel}\Omega) \times \exp[i\vec{Q}_{\parallel}\cdot(\vec{x}_{\parallel}-\vec{x}_{\parallel}') - i\Omega(t-t')] \ . \tag{2.2}$$

To calculate $S_{ij}(yy';\vec{Q}_{\parallel}\Omega)$ we examine the equation of motion for the closely related quantity, the dynamical susceptibility tensor $\chi_{ij}(\vec{x}\vec{x}';t-t')$, defined by the relation

$$\chi_{ij}(\vec{x}\vec{x}';t-t') = i\Theta(t-t')\langle[S_i(\vec{x},t),S_j(\vec{x}',t')]\rangle \ . \tag{2.3}$$

If the spin system is driven by an external magnetic field $h_i(\vec{x},t)$, then the expectation value $\langle S_i(\vec{x},t)\rangle$ of the spin-density operator is given by

$$\langle S_i(\vec{x},t)\rangle = \sum_j \int d^3x'\,dt'\,\chi_{ij}(\vec{x}\vec{x}';t-t')\,h_j(\vec{x}',t') \ . \tag{2.4}$$

It is easy to see that the Fourier transform $\chi_{ij}(yy';Q_{\parallel},\Omega+i\eta)$, defined in the manner of Eq. (2.2), is related to $S_{ij}(yy';\vec{Q}_{\parallel},\Omega)$ by the equation

$$S_{ij}(yy';\vec{Q}_{\parallel}\Omega) = i[1+n(\Omega)][\chi_{ij}(yy';\vec{Q}_{\parallel},\Omega+i\eta) - \chi_{ij}(yy';\vec{Q}_{\parallel},\Omega-i\eta)] \ , \tag{2.5}$$

where $n(\Omega) = [\exp(\hbar\Omega/k_BT)-1]^{-1}$ is the Bose-Einstein factor. It is useful to note the identity

$$\chi_{ij}(yy';\vec{Q}_{\parallel},\Omega-i\eta) = \chi_{ji}^{*}(y'y;\vec{Q}_{\parallel},\Omega+i\eta) \ , \tag{2.6}$$

which allows us to construct the correlation functions $S_{ij}(yy';\vec{Q}_{\parallel}\Omega)$ from quantities on only one side of the real axis in the complex Ω plane.

For the moment, since all quantities to be displayed below depend on $\vec{Q}_{\parallel}$ and Ω, we omit explicit reference to these variables. Then if n is the density of spins per unit volume, and S the magnitude of each spin, as in Ref. 7 we write

$$\chi_{xx}(y,y') = -nSg_{12}(y,y') \ , \tag{2.7a}$$

$$\chi_{xy}(y,y') = +nSg_{11}(y,y') \ , \tag{2.7b}$$

$$\chi_{yx}(y,y') = -nSg_{22}(y,y') \ , \tag{2.7c}$$

$$\chi_{yy}(y,y') = +nSg_{21}(y,y') \ . \tag{2.7d}$$

The differential equations satisfied by the functions $g_{ij}(y,y')$, when considered as functions of y for fixed y', are in fact identical to those which appear in Ref. 7. As before, with $\tilde{\Omega} = \Omega + i/\tau$, where τ is the transverse relaxation time of the spins, we may write (in appropriate units)

$$g_{11}(y,y') = \left[i\tilde{\Omega}\left[Q_{\parallel}^2 - \frac{\partial^2}{\partial y^2}\right] + 4\pi i M_s Q_x \frac{\partial}{\partial y}\right]\Lambda_1(y,y') \ , \tag{2.8a}$$

$$g_{21}(y,y') = \left[4\pi M_s Q_x^2 + \left[h - D\frac{\partial^2}{\partial y^2}\right]\left[Q_{\parallel}^2 - \frac{\partial^2}{\partial y^2}\right]\right] \times \Lambda_1(y,y') \ , \tag{2.8b}$$

while

$$g_{12}(y,y') = -\left[\left[h - D\frac{\partial^2}{\partial y^2}\right]\left[Q_{\parallel}^2 - \frac{\partial^2}{\partial y^2}\right] - 4\pi M_s \frac{\partial^2}{\partial y^2}\right] \times \Lambda_2(y,y') \tag{2.8c}$$

and

$$g_{22}(y,y') = i\left[\tilde{\Omega}\left[Q_{\parallel}^2 - \frac{\partial^2}{\partial y^2}\right] - 4\pi M_s Q_x \frac{\partial}{\partial y}\right] \times \Lambda_2(y,y') \ , \tag{2.8d}$$

where $h = H_0 + DQ_{\parallel}^2$, H_0 is the Zeeman field applied parallel to the magnetization M_s, along the z axis and D is the exchange stiffness constant.

Both $\Lambda_1(y,y')$ and $\Lambda_2(y,y')$ obey the same differential equation:

$$\left[\left[h - D\frac{\partial^2}{\partial y^2}\right]^2\left[Q_{\parallel}^2 - \frac{\partial^2}{\partial y^2}\right] - \tilde{\Omega}^2\left[Q_{\parallel}^2 - \frac{\partial^2}{\partial y^2}\right] + 4\pi M_s\left[h - D\frac{\partial^2}{\partial y^2}\right]\left[Q_x^2 - \frac{\partial^2}{\partial y^2}\right]\right] \times \Lambda_{1,2}(y,y') = \delta(y-y') \ . \tag{2.9}$$

The solution of Eq. (2.9) has the following form. First, if we consider the homogeneous version of Eq. (2.9), one has solutions of the form $\exp[\pm i\kappa y]$, where κ satisfies the equation

$$(h + D\kappa^2)^2(Q_{\parallel}^2 + \kappa^2) - \tilde{\Omega}^2(Q_{\parallel}^2 + \kappa^2) + 4\pi M_s(h + D\kappa^2)(Q_x^2 + \kappa^2) = 0 \ . \tag{2.10}$$

The roots of Eq. (2.10) denoted by κ_i where $i = 1, 2,$ or 3, are always complex, by virtue of the relaxation time τ included in the equations of motion. We choose κ_i so that

$$\mathrm{Im}(\kappa_i) > 0 \ . \tag{2.11}$$

In Ref. 7, it is demonstrated that Eq. (2.9) is satisfied by the choice

$$\Lambda_{1,2}(y,y') = \Lambda_{1,2}^{(\infty)}(y,y') = \frac{i}{2D^2}\sum_{i=1}^{3}\epsilon_i \exp(i\kappa_i|y-y'|) \tag{2.12}$$

where $\epsilon_1 = [\kappa_1(\kappa_1^2-\kappa_2^2)(\kappa_1^2-\kappa_3^2)]^{-1}$, and ϵ_2, ϵ_3 are obtained by permutation.

The Green's functions generated by the choice of $\Lambda_{1,2}(y,y')$ in Eq. (2.12) fail to satisfy the boundary conditions at $y=0$ and L. The full solution of our problem is found by adding solutions of the homogeneous version of Eq. (2.9) to the right-hand side of Eq. (2.12), then choosing the coefficients so the boundary conditions are satisfied. Thus, we write for y' fixed,

$$\Lambda_1(y,y') = \frac{i}{2D^2}\sum_{i=1}^{3}[\epsilon_i \exp(i\kappa_i|y-y'|) + \alpha_i^{(+)}\exp(+i\kappa_i y) + \alpha_i^{(-)}\exp(-i\kappa_i y)] , \tag{2.13}$$

where we shall find the coefficients $\alpha_i^{(+)}$ and $\alpha_i^{(-)}$ to be functions of y'. For $\Lambda_2(y,y')$, we have

$$\Lambda_2(y,y') = \frac{i}{2D^2}\sum_{i=1}^{3}[\epsilon_i \exp(i\kappa_i|y-y'|) + \beta_i^{(+)}\exp(i\kappa_i y) + \beta_i^{(-)}\exp(-i\kappa_i y)] . \tag{2.14}$$

The motion of the spins generates a demagnetizing field $\vec{h}_d(\vec{x},t)$, and as before we have calculated this in the magnetostatic approximation where $\vec{\nabla}\times\vec{h}_d(\vec{x},t)=0$, leading to $\vec{h}_d(\vec{x},t) = -\vec{\nabla}\phi_m(\vec{x},t)$, with $\phi_m(\vec{x},t)$ the potential from which the demagnetizing field is generated. As earlier, we encounter two additional Green's functions $g_{31}(y,y')$ and $g_{32}(y,y')$ which give the magnetostatic potential generated by the spin motions excited by the external driving field. We have not displayed the form of these functions here, since they do not enter our description of the light scattering process. They do enter the boundary conditions, however, and may be generated from $\Lambda_1(y,y')$ and $\Lambda_2(y,y')$ by relations similar to those in Eqs. (2.8).

Consider now the boundary conditions used to determine the coefficients $\alpha_i^{(+)}$ and $\alpha_i^{(-)}$. In addition to these six coefficients, the magnetic potential $\phi_m(\vec{x},t)$ is nonzero both above and below the film. This potential satisfies Laplace's equation in both regions, so we have $g_{31}(y,y') = \alpha_0^{<} e^{+Q_{\parallel}y}$ for $y<0$ and $g_{31}(y,y') = \alpha_0^{>} e^{Q_{\parallel}(L-y)}$ for $y>0$. Thus, we have eight undetermined coefficients in all. Continuity of normal components of $\vec{b}(\vec{x},t) = \vec{h}_d(\vec{x},t) + 4\pi \times \langle \vec{S}(\vec{x},t)\rangle$ at $y=0$ and L, combined with continuity of the magnetic potential provide four relations from which these constants may be determined. The form of the boundary conditions corresponds closely to those encountered in Ref. 7.

In addition, we impose spin pinning boundary conditions at $y=0$ and L that are similar to those used earlier. The boundary conditions read

$$\left.\frac{\partial g_{1i}(y,y')}{\partial y} - \lambda_< g_{1i}(y,y')\right|_{y=0+} = 0 , \tag{2.15a}$$

$$\left.\frac{\partial g_{2i}(y,y')}{\partial y} - \lambda_< g_{2i}(y,y')\right|_{y=0+} = 0 , \tag{2.15b}$$

while at $y=L$, we have

$$\left.\frac{\partial g_{1i}(y,y')}{\partial y} + \lambda_> g_{1i}(y,y')\right|_{y=L-} = 0 \tag{2.15c}$$

and

$$\left.\frac{\partial g_{2i}(y,y')}{\partial y} + \lambda_> g_{2i}(y,y')\right|_{y=L-} = 0 , \tag{2.15d}$$

where $i=1,2$.

A few brief comments on these conditions may prove helpful. If the constants $\lambda_<$ and $\lambda_>$ are chosen to be positive, the motion of spins in the respective surfaces are inhibited by effective pinning fields parallel to the externally applied Zeeman field. If one considers a semi-infinite fcc lattice of Heisenberg spins with a (100) surface, and takes the long-wavelength limit of the equations of motion under the assumption that spins in the surface "see" an effective magnetic field of strength H_s, then one finds boundary conditions of the form given in Eqs. (2.15) with $\lambda = a_0 H_s/2D$, where a_0 is the lattice constant. We shall later display a number of light scattering spectra calculated in the presence of pinning, where this formula allows one to estimate crudely the strength of the effective pinning fields from the values of λ used.

One assumption present in Eqs. (2.15) is that the effective surface pinning field acts parallel to (or possibly antiparallel to if either $\lambda_>$ or $\lambda_<$ are chosen negative) the externally applied Zeeman field. This need not be the case and the effective pinning field may well be noncolinear with the Zeeman field, with the consequence that spins are canted near the surface. It has been argued that such spin canting is present in the ferromagnetic resonance experiments of Yu *et al.*,[18] when the Zeeman field is applied in a general direction and is not parallel or perpendicular to the

surface.[19] It is not straightforward to modify the present formalism to include spin canting near the surface.

It may also be the case that pinning at the surface cannot be represented as a simple effective magnetic field parallel or antiparallel to the Zeeman field, even in the absence of canting near the surface. Quite generally, so long as the transverse magnetization can be described in macroscopic terms, we would expect boundary conditions of the form given in Eqs. (2.15) to be applicable, but the constants in the equations for $g_{1i}(y,y')$ need not be the same as those in the equations for $g_{2i}(y,y')$, i.e., the surface spins may wish to precess with an ellipticity that differs from that in the bulk. In our phenomenology, this effect may be incorporated by using in Eq. (2.15b) a value for $\lambda_<$ that differs from that which appears in Eq. (2.15a), and similarly for Eq. (2.15d). This modification is a trivial one but we have not explored it here because it increases the number of parameters that enter the theory. Instead, we shall try to provide the reader with a feeling for the relative importance of the contribution of spin motion parallel and perpendicular to the surface, in the various segments of the light scattering spectrum.

The solutions for the unknown coefficients α_i^+, α_i^-, β_i^+, and β_i^- are then obtained in a quite straight forward manner by applying these boundary conditions to the Green's functions g_{ij}. For completeness, we quote here the rather long and cumbersome resulting expressions for these quantities.

We introduce a 6×6 matrix $\underline{M}$, which is decomposed into four 3×3 submatrices as follows

$$\underline{M}=\begin{pmatrix}\underline{M}(++) & \underline{M}(+-)\\ \underline{M}(-+) & \underline{M}(--)\end{pmatrix} . \tag{2.16}$$

Below we have the explicit forms of the matrix elements,

$$M_{1i}(++)=(i\kappa_i-\lambda_<)\gamma_{1i}(+) , \tag{2.17a}$$

$$M_{2i}(++)=(i\kappa_i-\lambda_<)\gamma_{2i} , \tag{2.17b}$$

$$M_{3i}(++)=4\pi\gamma_{2i}+(Q_\parallel-i\kappa_i)\gamma_{3i}(+) , \tag{2.17c}$$

$$M_{1i}(+-)=-(i\kappa_i+\lambda_<)\gamma_{1i}(-)\exp(i\kappa_i L) , \tag{2.18a}$$

$$M_{2i}(+-)=-(i\kappa_i+\lambda_<)\gamma_{2i}\exp(i\kappa_i L) , \tag{2.18b}$$

$$M_{3i}(+-)=[4\pi\gamma_{2i}+(Q_\parallel+i\kappa_i)\gamma_{3i}(-)]\exp(i\kappa_i L) , \tag{2.18c}$$

$$M_{1i}(-+)=(i\kappa_i+\lambda_>)\gamma_{1i}(+)\exp(i\kappa_i L) , \tag{2.19a}$$

$$M_{2i}(-+)=(i\kappa_i+\lambda_>)\gamma_{2i}\exp(i\kappa_i L) , \tag{2.19b}$$

$$M_{3i}(-+)=[4\pi\gamma_{2i}-(Q_\parallel+i\kappa_i)\gamma_{3i}(+)]\exp(i\kappa_i L) , \tag{2.19c}$$

and finally

$$M_{1i}(--)=-(i\kappa_i-\lambda_>)\gamma_{1i}(-) , \tag{2.20a}$$

$$M_{2i}(--)=-(i\kappa_i-\lambda_>)\gamma_{2i} , \tag{2.20b}$$

$$M_{3i}(--)=4\pi\gamma_{2i}-(Q_\parallel-i\kappa_i)\gamma_{3i}(-) . \tag{2.20c}$$

In the above equations, we have defined

$$\gamma_{1i}(\pm)=-\frac{1}{2D^2}[\tilde{\Omega}(Q_\parallel^2+\kappa_i^2)\pm i4\pi M_s Q_x\kappa_i] , \tag{2.21a}$$

$$\gamma_{2i}=+\frac{i}{2D^2}[4\pi M_s Q_x^2+(h+D\kappa_i^2)(Q_\parallel^2+\kappa_i^2)] , \tag{2.21b}$$

and

$$\gamma_{3i}(\pm)=\frac{2\pi}{D^2}[i\tilde{\Omega}Q_x\pm\kappa_i(h+D\kappa_i^2)] . \tag{2.21c}$$

We need one more set of 3×3 matrices. These are $\underline{\Gamma}(+)$ and $\underline{\Gamma}(-)$, where the elements are given by

$$\Gamma_{1i}(+)=(i\kappa_i+\lambda_<)\gamma_{1i}(-)\epsilon_i , \tag{2.22a}$$

$$\Gamma_{2i}(+)=(i\kappa_i+\lambda_<)\gamma_{2i}\epsilon_i , \tag{2.22b}$$

and

$$\Gamma_{3i}(+)=-[4\pi\gamma_{2i}+(Q_\parallel+i\kappa_i)\gamma_{3i}(-)]\epsilon_i , \tag{2.22c}$$

also

$$\Gamma_{1i}(-)=-(i\kappa_1+\lambda_>)\gamma_{1i}(+)\epsilon_i\exp(i\kappa_i L) , \tag{2.23a}$$

$$\Gamma_{2i}(-)=-(i\kappa_i+\lambda_>)\gamma_{2j}\epsilon_i\exp(i\kappa_i L) , \tag{2.23b}$$

and

$$\Gamma_{3i}(-)=[-4\pi\gamma_{2i}+(Q_\parallel+i\kappa_i)\gamma_{3i}(+)]\epsilon_i\exp(i\kappa_i L) . \tag{2.23c}$$

Then if $\underline{N}=\underline{M}^{-1}$, we have the forms

$$\alpha_i^{(+)}=\sum_{j=1}^{3}\sum_{k=1}^{3}N_{ij}(++)\Gamma_{jk}\exp(+i\kappa_k y')+\sum_{j=1}^{3}\sum_{k=1}^{3}N_{ij}(+-)\Gamma_{jk}(-)\exp(-i\kappa_k y') \tag{2.24a}$$

and

$$\alpha_i^{(-)}=\sum_{j=1}^{3}\sum_{k=1}^{3}N_{ij}(-+)\Gamma_{jk}(+)\exp(i\kappa_k y')+\sum_{j=1}^{3}\sum_{k=1}^{3}N_{ij}(--)\Gamma_{jk}(-)\exp(-i\kappa_k y') . \tag{2.24b}$$

We require similar expressions for β_i^+ and β_i^-. Again, for completeness, we give without derivation the formulas required for this purpose. We have now in place of $\underline{M}$, a matrix $\underline{P}$ which when broken up into 3×3 blocks has the form

$$P_{1i}(++)=(i\kappa_i-\lambda_<)\delta_{2i}(+) \ , \tag{2.25a}$$

$$P_{2i}(++)=(i\pi_i-\lambda_<)\delta_{1i} \ , \tag{2.25b}$$

$$P_{3i}(++)=4\pi\delta_{2i}(+)+(Q_\parallel-i\kappa_i)\delta_{3i}(+) \ , \tag{2.25c}$$

$$P_{1i}(+-)=-(i\kappa_i+\lambda_<)\delta_{2i}(-)\exp(i\kappa_i L) \ , \tag{2.26a}$$

$$P_{2i}(+-)=-(i\kappa_i+\lambda_<)\delta_{1i}\exp(i\kappa_i L) \ , \tag{2.26b}$$

and

$$P_{3i}(+-)=[4\pi\delta_{2i}(-)+(Q_\parallel+i\kappa_i)\delta_{3i}(-)]\exp(i\kappa_i L) \ . \tag{2.26c}$$

Also

$$P_{1i}(-+)=(i\kappa_i+\lambda_>)\delta_{2i}(+)\exp(i\kappa_i L) \ , \tag{2.27a}$$

$$P_{2i}(-+)=(i\kappa_i+\lambda_>)\delta_{1i}\exp(i\kappa_i L) \ , \tag{2.27b}$$

and

$$P_{3i}(-+)=[4\pi\delta_{2i}(+)-(Q_\parallel+i\kappa_i)\delta_{3i}(+)]\exp(i\kappa_i L) \ . \tag{2.27c}$$

While

$$P_{1i}(--)=-(i\kappa_i-\lambda_>)\delta_{2i}(-) \ , \tag{2.28a}$$

$$P_{2i}(--)=-(i\kappa_i-\lambda_>)\delta_{1i} \ , \tag{2.28b}$$

and

$$P_{3i}(--)=4\pi\delta_{2i}(-)-(Q_\parallel-i\kappa_i)\delta_{3i}(-) \ . \tag{2.28c}$$

We have for δ_{1i}, $\delta_{2i}(\pm)$, and $\delta_{3i}(\pm)$,

$$\delta_{1i}=-\frac{i}{2D^2}[4\pi M_s\kappa_i^2+(h+D\kappa_i^2)(Q_\parallel^2+\kappa_i^2)] \ , \tag{2.29a}$$

$$\delta_{2i}(\pm)=-\frac{1}{2D^2}[\tilde{\Omega}(Q_\parallel^2+\kappa_i^2)\mp i4\pi M_s Q_x\kappa_i] \ , \tag{2.29b}$$

and

$$\delta_{3i}(\pm)=-\frac{2\pi}{D^2}[Q_x(h+D\kappa_i^2)\mp i\tilde{\Omega}\kappa_i] \ . \tag{2.29c}$$

Finally, we need the matrices $\underline{\Delta}(+)$ and $\underline{\Delta}(-)$, where

$$\Delta_{1i}(+)=(i\kappa_i+\lambda_<)\delta_{2i}(-)\epsilon_i \ , \tag{2.30a}$$

$$\Delta_{2i}(+)=(i\kappa_i+\lambda_<)\delta_{1i}(-)\epsilon_i \ , \tag{2.30b}$$

$$\Delta_{3i}(+)=-[4\pi\delta_{2i}(-)+(Q_\parallel+i\kappa_i)\delta_{3i}(-)]\epsilon_i \ , \tag{2.30c}$$

and

$$\Delta_{1i}(-)=-(i\kappa_i+\lambda_>)\delta_{2i}(+)\epsilon_i\exp(i\kappa_i L) \ , \tag{2.31a}$$

$$\Delta_{2i}(-)=(i\kappa_i+\lambda_>)\delta_{1i}\epsilon_i\exp(i\kappa_i L) \ , \tag{2.31b}$$

$$\Delta_{3i}(-)=[4\pi\delta_{2i}(+)-(Q_\parallel+i\kappa_i)\delta_{3i}(+)]\epsilon_i\exp(i\kappa_i L) \tag{2.31c}$$

Then if $\underline{Q}=\underline{P}^{-1}$, we have finally

$$\beta_i^{(+)}=\sum_{j=1}^{3}\sum_{k=1}^{3}Q_{ij}(++)\Delta_{jk}(+)\exp(+i\kappa_k y')+\sum_{j=1}^{3}\sum_{k=1}^{3}Q_{ij}(+-)\Delta_{jk}(-)\exp(-i\kappa_k y') \tag{2.32a}$$

and

$$\beta_i^{(-)}=\sum_{j=1}^{3}\sum_{k=1}^{3}Q_{ij}(-+)\Delta_{jk}(+)\exp(i\kappa_k y')+\sum_{j=1}^{3}\sum_{k=1}^{3}Q_{ij}(--)\Delta_{jk}(-)\exp(-i\kappa_k y') \ . \tag{2.32b}$$

We apologize to the reader for these lengthy expressions but we feel it necessary to write them since the Green's functions defined above can be applied to a variety of calculations other than that of the light scattering spectrum of the film.

We now have in hand the results required to calculate the spectral density functions $S_{ij}(yy';\vec{Q}_\parallel\Omega)$ defined in Eq. (2.5). In Sec. III, we discuss how these are related to the light scattering spectrum of the film.

III. LIGHT SCATTERING BY SPIN FLUCTUATIONS IN FERROMAGNETS

In Sec. II we concentrated on the method used to generate the spin-correlation functions that describe thermal fluctuations in the spin system, we now turn to a description of light scattering (Brillouin scattering) by these fluctuations.

When the spins fluctuate about their equilibrium orientation, the (complex) dielectric function of the material is modulated. Thus, for a material of cubic symmetry, the time-dependent dielectric tensor $\epsilon_{\mu\nu}(\vec{x},t)$, in the presence of spin fluctuations, may be written

$$\epsilon_{\mu\nu}(\vec{x},t)=\epsilon_0\delta_{\mu\nu}+\delta\epsilon_{\mu\nu}(\vec{x},t) \ , \tag{3.1}$$

where ϵ_0 is the complex dielectric constant and the fluctuating part, according to Landau and Lifshitz,[20]

has the form

$$\delta\epsilon_{\mu\nu}(\vec{x},t)=\delta\epsilon_{\mu\nu}^{(1)}(\vec{x},t)+\delta\epsilon_{\mu\nu}^{(2)}(\vec{x},t)+\cdots \tag{3.2a}$$

and

$$\delta\epsilon_{\mu\nu}^{(1)}(\vec{x},t)=\sum_{\lambda}K_{\mu\nu\lambda}S_{\lambda}(\vec{x},t)\ , \tag{3.2b}$$

$$\delta\epsilon_{\mu\nu}^{(2)}(\vec{x},t)=\sum_{\lambda\delta}G_{\mu\nu\lambda\delta}S_{\lambda}(\vec{x},t)S_{\delta}(\vec{x},t)\ . \tag{3.2c}$$

The light is scattered inelastically by the time and spatial variations in the dielectric tensor. In recent years, methods have been developed that allow one to relate the Brillouin scattering cross section for back scattering from an opaque substrate or film to certain averages over the spin-correlation functions $S_{ij}(yy';\vec{Q}_{\parallel}\Omega)$ analyzed in Sec. II. These methods, along with a number of applications are reviewed in Ref. 4, and their application to light scattering from a ferromagnetic material, semi-infinite in extent, has been discussed in Ref. 7. As a result, we comment only briefly on these procedures in Sec. IV, and here we turn to certain important aspects of this process which we did not discuss in detail earlier.

To begin with we recall the description of light scattering from spin waves in nominally transparent media. Here the light penetrates deeply, and the bulk spin waves, which provide the dominant contribution to the cross section can be regarded as plane-wave excitations in a medium of infinite spatial extent. To an excellent approximation the incident and scattered photon can also be treated as plane waves. A complete and early treatment of this problem has been given by Le Gall and his collaborators,[21] and more recently Wettling, Cottam, and Sandercock[22] have presented a careful and quantitative analysis of their data on the light scattering from bulk spin waves in YIG.

These papers illustrate that for the Brillouin scattering of the incident photon by one magnon processes, both $\delta\epsilon_{\mu\nu}^{(1)}(\vec{x},t)$ *and* $\delta\epsilon_{\mu\nu}^{(2)}(\vec{x},t)$ contribute to the cross section. The term $\delta\epsilon_{\mu\nu}^{(1)}(\vec{x},t)$ enters because for a cubic material the $K_{\mu\nu\lambda}$ in Eq. (3.2b) has the form

$$K_{\mu\nu\lambda}=iK\epsilon_{\mu\nu\lambda}\ , \tag{3.3}$$

where K is a purely real constant in the absence of absorption. From Eq. (3.2b) it then follows that one magnon terms proportional to $S_x(\vec{x},t)$ and $S_y(\vec{x},t)$ contribute to $\delta\epsilon_{zy}^{(1)}(\vec{x},t)$ and $\delta\epsilon_{zx}^{(1)}(\vec{x},t)$, respectively. There are also such one magnon terms in $\delta\epsilon_{\mu\nu}^{(2)}(\vec{x},t)$ which interfere coherently with those in $\delta\epsilon_{\mu\nu}^{(1)}(\vec{x},t)$. These come from the $S_z(\vec{x},t)S_x(\vec{x},t)$ and $S_z(\vec{x},t)S_y(\vec{x},t)$ terms in Eq. (3.2c) which, in the spin wave regime become $nSS_x(\vec{x},t)$ and $nSS_y(\vec{x},t)$, respectively, where n is the number of spins per unit volume. Let $G_{44}=G_{zxzx}$, and introduce the spin raising and lowering operators $S_{\pm}(\vec{x},t)=S_x(\vec{x},t)\pm iS_y(\vec{x},t)$, such that

$$\delta\epsilon_{zx}(\vec{x},t)=\tfrac{1}{2}(K+nSG_{44})S_{+}(\vec{x},t)+\tfrac{1}{2}(K-nSG_{44})S_{-}(\vec{x},t)\ , \tag{3.4}$$

with a similar expression for $\delta\epsilon_{zy}(\vec{x},t)$.

If we now consider a Stokes process, where a spin wave is created in the light scattering event, from Eq. (3.4) we see that the matrix element is proportional to $|K-nSG_{44}|^2$. Conversely, for an anti-Stokes process, the matrix element is instead proportional to $|K+nSG_{44}|^2$. Thus, as Le Gall and co-workers first pointed out,[21] the ratio of the Stokes intensity to that of the anti-Stokes can differ dramatically from the often quoted value $\exp(\hbar\Omega/k_BT)$. In the presence of ferromagnetic order, the breakdown of time reversal symmetry resulting from the replacement of $S_z(\vec{x},t)$ by $+nS$, allow the Stokes/anti-Stokes ratio to deviate from the value of $\exp(\hbar\Omega/k_BT)$, which is very close to unity for frequencies in the Brillouin range.[23] A quantitative comparison between the data on Brillouin scattering from spin waves in YIG, and the Stokes and anti-Stokes intensities deduced from the above coupling mechanism, has been provided by Wettling, Cottam, and Sandercock.[22]

In our studies of the Brillouin spectra for light scattering from spin waves in the ferromagnetic metals, we have found very good fits to the experimental spectra from analyses which include only the terms in $\delta\epsilon_{\mu\nu}^{(1)}(\vec{x},t)$. We give an example of this in Fig. 3, where we compare a Brillouin spectrum calculated for scattering off of spin waves near the surface of a semi-infinite sample of Fe with the data reported by Sandercock.[24] In the notation of Fig. 2, the data are taken for a geometry with $\phi_s=0$, and $\theta_0=\theta_s=45°$;

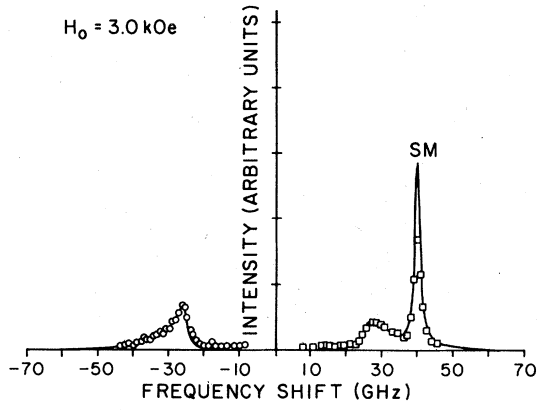

FIG. 3. Comparison between the calculated and measured Brillouin spectra for scattering from the surface of Fe. The g factor has been taken equal to 2.09, and the exchange constant $D=2.5\times10^{-9}$ Oe cm^2. The surface wave peak is denoted by SM.

i.e., the scattered photon has wave vector $\vec{k}^{(s)} = -\vec{k}^{(0)}$, where $\vec{k}^{(0)}$ is the wave vector of the incident photon. Without invoking the terms quadratic in the spin density, we obtain an excellent fit to the data.

The features that appear in this spectrum have been discussed in detail in the earlier papers, but we remind the reader that the peak SM on the Stokes side of the spectrum has its origin in scattering from the Damon-Eshbach surface spin wave. We have a line on only one side of the laser line because the Damon-Eshbach wave is a curious "one way" surface wave, which can propagate from left to right across the magnetization, but not from right to left. The asymmetric band on each side of the laser line is by scattering from bulk spin waves; we have a continuous band of frequencies in the spectrum because the skin depth is small, and the wave-vector components normal to the surface are not conserved in the scattering process,[4] though those parallel to it are. For each direction of the scattered photon, the kinematics allow scatterings produced by all bulk spin waves with wave-vector projection on the surface equal to $\vec{k}_{\parallel}^{(0)} - \vec{k}_{\parallel}^{(s)}$, leading to a continuous band of frequencies from the bulk spin waves with intensity controlled by the matrix element which couples light to the various waves. A qualitative discussion of the shape of such spectra has been presented recently.[4]

From Fig. 3, one sees very clearly that there is a difference between the shape and intensity of the bulk spin-wave contributions to the Stokes side of the spectrum, and those to the anti-Stokes side. Note that, for the particular geometry employed by Sandercock, the differences are subtle, though clearly discernable in both the theory and the data. We shall show spectra below which are calculated for a different geometry and in which, like the data on the thin films,[2] a much more pronounced asymmetry is present.

Since we have ignored the contributions to $\delta\epsilon_{\mu\nu}(\vec{x},t)$ quadratic in the spin density, the mechanism responsible for the bulk spin-wave Stokes–anti-Stokes asymmetries in Fig. 3 is clearly different from the interference effect discussed above. We have here, in our view, an example of a surface effect which modifies the Stokes–to–anti-Stokes ratio for scattering from bulk spin waves. We argue below that it is the breakdown of a certain reflection symmetry in the presence of the surface rather than that of time-reversal symmetry, as in the interference phenomenon reviewed above, that produces this effect.

In a number of previous papers, it has been noted that the dispersion relation for surface spin waves on ferromagnets with magnetization parallel to the surface are nonreciprocal in character, i.e., $\Omega_s(+\vec{Q}_{\parallel}) \neq \Omega_s(-\vec{Q}_{\parallel})$. The Damon-Eshbach wave which appears in the spectrum of Fig. 3 is an extreme example of such a mode, since the wave exists only for one unique sense of propagation across the magnetization. Nonreciprocal behavior is also found for surface magnetoelastic waves which propagate on ferromagnets,[25] and for surface polaritons which propagate on doped semiconductors placed in a magnetic field parallel to the surface.[26] One's first guess is that a breakdown in time-reversal symmetry is also responsible for this very striking property of the surface waves. Such a breakdown should also affect the dispersion relation of the bulk waves in the infinitely extended medium but in fact in all cases, the dispersion relation of the corresponding bulk waves contains no hint of nonreciprocal behavior.

We have already alluded to a breakdown of reflection symmetry produced by the surface that leads to the nonreciprocal properties of the surface waves. Consider the geometry of Fig. 2, and let $\hat{R}_{ij}$ denote the operation of reflection through the plane which contains the pair of Cartesian axes i and j. Then in the infinitely extended medium, when due account is taken of the axial vector character of the magnetization, $\hat{R}_{xz}$ and $\hat{R}_{yz}$ are not good symmetry operations, but the product $\hat{R}_{xz}\hat{R}_{yz}$ is. For waves in the infinitely extended medium, the existence of this symmetry operation combined with $\hat{R}_{xy}$ is sufficient to prove that $\Omega_B(+\vec{Q}) = \Omega_B(-\vec{Q})$, where $\Omega_B(\vec{Q})$ is the dispersion relation of any bulk excitation. Now if we place ourselves near the surface of semi-infinite ferromagnet, with axes oriented as in Fig. 2, then $\hat{R}_{xz}\hat{R}_{yz}$ is no longer a good symmetry operation, and there is no symmetry operation which requires $\Omega_s(+\vec{Q}_{\parallel})$ and $\Omega_s(-\vec{Q}_{\parallel})$ to be equal.

Consider a semi-infinite material, and examine a bulk spin wave far from the surface of wave vector $\vec{Q}$. If this wave propagates to the surface and is reflected from it with $R(\vec{Q}_{\parallel})$ the reflection coefficient, the symmetry argument above shows that $R(+\vec{Q}_{\parallel})$ will not equal $R(-\vec{Q}_{\parallel})$. It follows that the *eigenvector* of a bulk spin-wave eigenmode of the semi-infinite medium with frequency Ω and wave vector $+\vec{Q}_{\parallel}$ in the plane parallel to the surface will differ from that of a bulk spin wave with frequency Ω and wave vector $-\vec{Q}_{\parallel}$. It is these differences in the *eigenvectors* of the bulk wave, traceable to differences in the reflection coefficients, that are responsible for the Stokes–anti-Stokes asymmetries in the bulk spin-wave contributions to the theoretical spectrum displayed in Fig. 3, and in the remainder of the paper. The Stokes–anti-Stokes asymmetries in the bulk spin-wave regions of the spectra are not due to the interference effect invoked in earlier analyses of Brillouin scattering from spin waves in nominally transparent media, but rather to the same breakdown of reflection symmetry that is responsible for the nonreciprocal character of the surface wave dispersion relation. We call the reader's attention to a recent theoretical study by Laks and Mills[27] of the reflection

coefficient for reflection of bulk magnetoelastic waves from the surface of a semi-infinite ferromagnet. The analysis shows explicitly, for a different physical situation, asymmetry in the reflection coefficient identical to that described here.

In the light of the above remarks, it is interesting to examine the theoretical calculations in Ref. 7. In the first paper, a series of calculations of the Brillouin scattering of light from spin waves near the surface of Fe and EuO were reported. The skin depth for Fe is roughly 150 Å, for the optical constants employed in this work, and the Stokes–anti-Stokes asymmetry in the bulk spin-wave portions of the spectrum is evident, though as in Fig. 3 of the present paper, it is subtle. On the other hand, the calculations carried out for scattering from spin waves in EuO, with $G_{\mu\nu\lambda\delta} \equiv 0$, show no asymmetry at all, at least to graphical accuracy. Here, the skin depth being 1500 Å the light penetrates deeply enough that the influence of the surface on the bulk spin-wave eigenvectors has little effect on the calculated spectra. In contrast, the data of Grünberg and Metawe[3] shows a very large Stokes–anti-Stokes asymmetry in the bulk spin-wave contributions to the backscattering spectra. In this case, as the second series of calculations reported in Ref. 7 illustrate, it is interference between the terms in $K_{\mu\nu\lambda}$ and $G_{\mu\nu\lambda\delta}$ that is responsible for the asymmetry.

We conclude that in Brillouin studies of the backscattering of light from spin waves near the surface of strongly absorbing media, there are in principle two distinct sources of Stokes–anti-Stokes asymmetry in the bulk spin-wave spectra of the material. The first is the interference effect pointed out by Le Gall and co-workers,[21] which was employed in an elegant fashion by Wettling, Cottam, and Sandercock[22] in their interpretation of the data on light scattering from spin waves in YIG. This interference is also the dominant source of the asymmetries found by Grünberg and Metawe in their work on EuO. The other is that in the absence of the interference effect, very appreciable Stokes–anti-Stokes asymmetries can be produced by an intrinsic surface effect, which renders the eigenvectors of spin waves in a semi-infinite medium (or film, of course) with wave vector $\vec{Q}_{\parallel}$ inequivalent to those with wave vector $-\vec{Q}_{\parallel}$. Our calculations show it is the second effect which is the dominant source of the asymmetry in the ferromagnetic metals examined so far.

Both $K_{\mu\nu\lambda}$ and $G_{\mu\nu\lambda\delta}$ may be measured directly by optical means, as Wettling *et al.* have emphasized,[22] and the interpretation of light scattering spectra would be assisted greatly by such measurements though this may be a difficult task for materials with small skin depths. The tensor $K_{\mu\nu\lambda}$ controls the Faraday rotation of light, while the quadratic terms control the Cotton-Mouton effect. While one cannot propagate radiation through samples with small skin depths, unless very thin samples are employed, the polarization properties of light reflected from the surface is also affected by the presence of the terms in $\epsilon_{\mu\nu}$ proportional to $K_{\mu\nu\lambda}$ and $G_{\mu\nu\lambda\delta}$. Thus, suitable studies of the reflectivity of the ferromagnetic metals would be most useful.

IV. RESULTS OF THE NUMERICAL CALCULATIONS

In this section, we present the results of our numerical calculations on spin waves in thin films. We begin first with a summary of how the calculations are performed.

In Sec. III, we saw that thermal fluctuations in the spin system modulates the dielectric tensor of the medium. As in earlier treatments,[4,7] the scattered field $E_{\alpha}^{(s)}(\vec{x},t)$ may be written, to first order in $\delta\epsilon_{\mu\nu}(\vec{x},t)$

$$E_{\alpha}^{(s)}(\vec{x},t) = \left(\frac{\omega_0}{c}\right)^2 \sum_{\beta\gamma} \int \frac{d^3x'\,dt'}{4\pi} D_{\alpha\beta}(\vec{x}\vec{x}';t-t') \times \delta\epsilon_{\beta\gamma}(\vec{x}',t') E_{\gamma}^{(0)}(\vec{x}',t') \,. \tag{4.1}$$

In Eq. (4.1), $E_{\gamma}^{(0)}(\vec{x},t')$ is the electric field associated with the incident photon, $\delta\epsilon_{\beta\gamma}(\vec{x},t)$ was discussed in Sec. III, and the $D_{\alpha\beta}(\vec{x}\vec{x}';t-t')$ are Green's functions for Maxwell's equations applied to a film of thickness L, dielectric constant ϵ_0 and placed in vacuum. The explicit form of these Green's functions have been given elsewhere,[28] along with the prescription for forming the Brillouin cross section from the scattered fields in Eq. (4.1).[7]

In all the calculations for the scattering of photons from films of Fe and amorphous $Fe_{80}B_{20}$ that we report here, we have used for the incident field $E_{\gamma}^{(0)}(\vec{x},t)$ and the Green's function $D_{\alpha\beta}(\vec{x}\vec{x}',t-t')$ the forms appropriate for a semi-infinite medium. This is a good approximation for the films considered here since their optical skin depth δ, which is roughly 150 Å, is small compared to the film thickness. The use of the full forms greatly complicates the algebra, and the above approximations have little quantitative influence on the results presented here. We also remind the reader that we have included only the contribution $\delta\epsilon_{\mu\nu}^{(1)}(\vec{x},t)$ to the dielectric tensor since, as illustrated in Fig. 3, for the ferromagnetic transition metals the spectra can be fitted well with only this term. The optical constants have been taken as $n = 2.86$ and $\kappa = 2.91$.

In Fig. 4, we show calculations of the spectra for back scattering of light from Fe films of various thicknesses. The scattering geometry is the same as that chosen for Fig. 3 and used in the experimental work of Sandercock *et al.* Both the incident and the

scattered photon have wave vectors that lie in the xy plane, and the wave vector $\vec{k}_s$ of the scattered photon is antiparallel to the wave vector $\vec{k}_0$ of the incident photon. The angle of incidence θ_0 is 45°, the electric field of the incident photon is parallel to the magnetization, and that of the scattered photon then necessarily lies in the xy plane.

The most prominent feature in Fig. 4 is the strong line from the Damon-Eshbach surface spin wave in each of the spectra. In addition, the broad band produced by scattering from the bulk spin waves now breaks up into a sequence of discrete peaks corresponding to scattering from standing spin-wave resonances of the thin film. These calculations assume the spins in the surface to be unpinned and illustrate clearly the point made in Sec. I that, while in microwave studies of thin films only the uniform mode absorbs with appreciable intensity, the light scattering method allows one to see an entire sequence of standing spin waves.

Since the light illuminates only the surface near $y=0$, the Damon-Eshbach surface wave is that which propagates on the upper surface. In the thinnest film explored in Fig. 4, we see a surface wave feature on *both* sides of the laser line. The weak surface feature on the anti-Stokes side of the line appears because the film is thin enough for the surface wave on the lower surface of the film to contribute to the spectrum, with appreciable intensity. When the film is viewed from above, the mode localized primarily on the upper surface propagates from left to right across the magnetization, and that localized primarily on the lower surface propagates from right to left. A consequence is that the scattering geometry places the mode on the upper surface on the Stokes side of the spectrum, that on the lower surface appears on the anti-Stokes side. One can thus discriminate between the two, and the study of these modes should prove to be a useful way of characterizing each of the interfaces of a thin film. Spectra taken on films sufficiently thin to display both surface waves have been reported by Camley and Grimsditch.[6] The authors have used the formalism developed here, to obtain results which seem to account for the observed intensities very well.

We can obtain a feeling for the relative importance of scattering from spin motions normal to or parallel to the surface by exploring the spectral density functions $S_{ij}(\vec{Q}_{\parallel}\Omega;yy')$ directly. In Fig. 5, we show plots of $S_{xx}(\vec{Q}_{\parallel}\Omega;yy)$ and $S_{yy}(\vec{Q}_{\parallel}\Omega,yy)$ as a function of frequency for fixed value of $\vec{Q}_{\parallel}$ (here $Q_{\parallel}L=1.5188$ with L as the film thickness). We assume the spins to be unpinned and put $y=0$; the plots of the functions for the surface at $y=L$ are exact mirror images of these. The physical interpretation of the functions is as follows. Imagine a slab of material of thickness dy, with surfaces parallel to the surface of our film. If one samples the thermal spin fluctuations parallel to the surface, and takes the Fourier transform with respect to $\vec{x}_{\parallel}$ and time, then $S_{xx}(\vec{Q}_{\parallel}\Omega;yy)$ is a measure of the square of the amplitude of the spin fluctuations with frequency Ω, and wave vector $\vec{Q}_{\parallel}$ parallel to the surface. In a similar fashion, $S_{yy}(\vec{Q}_{\parallel}\Omega;yy)$ is a measure of the amplitude of the spin fluctuations perpendicular to the surfaces. Thus, by scanning $S_{xx}(\vec{Q}_{\parallel}\Omega;yy)$ and $S_{yy}(\vec{Q}_{\parallel}\Omega;yy)$ as a function of y, we can learn about the spatial distribution of the spin fluctuations that contribute to the light scattering spectrum. For example, from Fig. 5, one sees that the Damon-

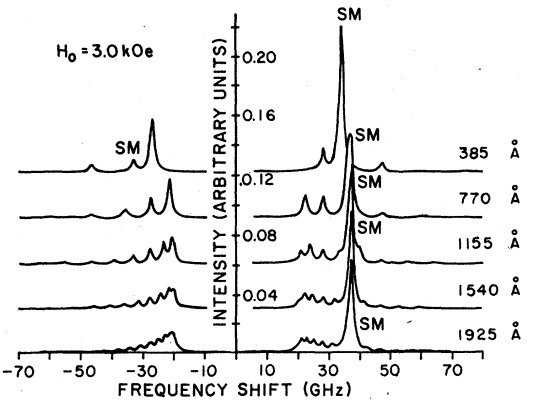

FIG. 4. Several spectra calculated for the backscattering of light from Fe film of various thicknesses. The scattering geometry and parameters are identical to those used for Fig. 3. The features labeled with an SM are produced by scattering from the Damon-Eshbach surface spin wave.

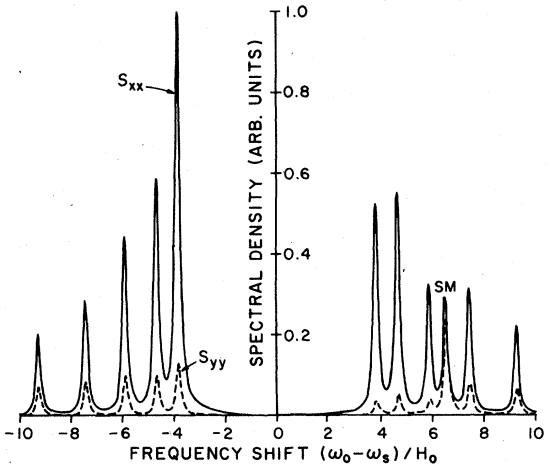

FIG. 5. Calculations of $S_{xx}(\vec{Q}_{\parallel}\Omega,yy)$ and $S_{yy}(\vec{Q}_{\parallel}\Omega,yy)$ for $y=0$ for a film of Fe with thickness of 880 Å. We have chosen $Q_{\parallel}L=1.5188$, $1/\tau=0.15H_0$, the Zeeman field $H_0=1.9$ kOe, and $D=2.5\times10^{-9}$ Oe cm^2.

Eshbach surface wave feature contributes roughly equally to both $S_{xx}(\vec{Q}_{\parallel}\Omega;yy)$ and $S_{yy}(\vec{Q}_{\parallel}\Omega;yy)$. In fact, in the absence of exchange and for propagation perpendicular to the magnetization, the wave is strictly circularly polarized for propagation perpendicular to the magnetization, as in Fig. 5. The small difference between the two features is presumably an effect of including exchange in the calculation.

This result implies that the dominant contribution to the Damon-Eshbach feature in the light scattering spectrum comes from spin fluctuations *normal* to the surface. This is because regardless of the direction of propagation of the incident or scattered photon (unless it is nearly parallel to the surface), the electric field in the medium is always nearly parallel to the surface. To see this note that $\vec{\nabla}\cdot\vec{E}=0$ inside the metal implies $|E_{\parallel}/E_{\perp}|=|k_{\perp}/k_{\parallel}|$, where $E_{\parallel}$ and $E_{\perp}$ are the components of the electric field parallel and perpendicular to the surface, respectively, and $k_{\perp}$ and $k_{\parallel}$ are the components of the wave vector normal to and parallel to the surface. Since $k_{\parallel}=\omega\sin\theta/c$ and $k_{\perp}=\omega(\epsilon-\sin^2\theta)^{1/2}/c$, where θ is the angle between the propagation direction and the normal to the film surface, it follows that for our choice of the optical constants the ratio $|E_{\parallel}/E_{\perp}|$ varies from 5 to 10. With the electric field nearly parallel to the film surface, the tensor $K_{\mu\nu\lambda}$ given in Eq. (3.3), couples the light primarily to the spin fluctuations perpendicular to the film surface. (Note that one of the two photons in the scattering event must have a nonzero component of the electric field in the z direction.)

On the other hand, we find that the contribution from the bulk spin waves to $S_{xx}(\vec{Q}_{\parallel}\Omega;yy)$ is larger than that to $S_{yy}(\vec{Q}_{\parallel}\Omega;yy)$ by roughly an order of magnitude. Moreover the surface demagnetizing field causes the spin precession in the standing spin-wave eigenvectors to be highly elliptical, with the major axis aligned parallel to the film surface. The result is that the ratio $(E_{\parallel}S_{yy}/E_{\perp}S_{xx})$ is close to unity, hence the cross section for light scattering has comparable contributions from spin fluctuations parallel and perpendicular to the film surface.

The conclusions of the previous paragraph are valid only when $H_0/4\pi M_s$ is less than unity as the degree of ellipticity present in the bulk spin waves depends on this ratio. In particular, if $H_0 >> 4\pi M_s$, the spin precession associated with the bulk spin waves is nearly circular in character. In the regime where the spin precession in the bulk spin waves is highly elliptical, as in the example displayed in Fig. 5, anisotropic pinning [i.e., a boundary condition of the form given in Eq. (2.15) with $\lambda_>$ and $\lambda_<$ different for the x and y components of the transverse magnetization] will affect the *relative* intensity of the surface and bulk wave features in the light scattering spectrum. We have not considered this here but it should be possible to use this as a test of isotropic pinning boundary condition.

The functions $S_{xx}(\vec{Q}_{\parallel},-\Omega,LL)$ and $S_{yy}(\vec{Q}_{\parallel},-\Omega;LL)$ are identical to $S_{xx}(\vec{Q}_{\parallel}\Omega;00)$ and $S_{yy}(\vec{Q}_{\parallel}\Omega;00)$, respectively. This is a consequence of the fact that for a film of finite thickness, the combination of reflection operations $R_{xz}R_{yz}$ is a good symmetry operation, provided the R_{yz} reflection is taken about the midpoint of the film. We can see that when the light penetrates deeply enough to sample the film surface at $y=L$, the surface wave on the lower surface appears on the side of the laser line opposite to the position of the surface wave localized on the upper surface.[29]

In Fig. 5 we had fixed the value of $\vec{Q}_{\parallel}$ and y and plotted the spectral density as a function of the frequency Ω. In Fig. 6, we obtain a feeling for the eigenvector of the various modes by fixing Ω and $\vec{Q}_{\parallel}$ suitably and plotting the spectral density as a function of the depth y. For fixed $\vec{Q}_{\parallel}$, we set the frequency Ω equal to that of the mode whose eigenvector is desired. Then a plot of $S_{xx}(\vec{Q}_{\parallel}\Omega;yy)$ as a function of y gives us the *square* of the eigenvector associated with the x component of the spin motion in the mode, and similarly for $S_{yy}(\vec{Q}_{\parallel}\Omega;yy)$. For this graph we use the same parameters as in Fig. 5. The

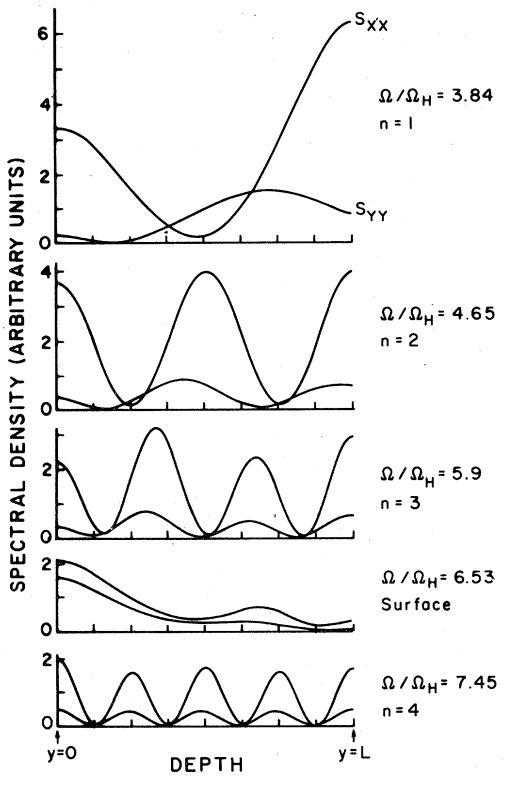

FIG. 6. Spectral density vs depth for the peaks seen in Fig. 5.

graph shows the rather large differences between the real modes in a ferromagnetic slab with $\vec{Q}_{\parallel} \neq 0$ and the idealized ones drawn in Fig. 1. There are several interesting features in Fig. 6: (a) for this geometry, and for propagation perpendicular to the field, there is no $n=0$ mode; (b) the nodes for S_{xx} and S_{yy} for the first few modes do not occur at the same depth; and (c) the spatial profile of the surface mode is not a simple dying exponential, but we see explicitly some mixing with the bulk modes. In the limit the sample becomes semi-infinite, this leads to the "leaky" character of the Damon-Eshbach wave discussed in Ref. 7.

The calculations presented above are intended to provide the reader with an overview of the basic physics of light scattering from spin waves in films. Now we turn to a series of calculations directed toward the data reported by Grimsditch, Malozemoff, and Brunsch.[2] We adopt the geometry used in their experiment and the value for the exchange constant $D=1.4\times10^{-9}$ Oe cm^2 deduced by them from their data. The film thickness L has been taken to be 1060 Å. In the experiments, both the incident and scattered photon lie in the xy plane, so $\phi_s=0$, the angle of incidence θ_0 of the incoming photon is 59°, and the scattered photon emerges along the normal to the film. The calculations serve to illustrate the influence of spin pinning on the spectrum.

In Fig. 7, we show the spectrum calculated for the case where no spin pinning is present. The spectrum bears a striking resemblance to the data. The Damon-Eshbach wave is by far the strongest feature in the calculated spectrum, as it is in the data. Similarly, the experiments show the relative intensity of the S_1, S_2, and S_3 bulk magnons to alternate as in the figure, while the anti-Stokes features have monotonically decreasing intensity. (To see this in the data, one must recognize that the peaks labeled A_3 and A_4 in Fig. 2 of Ref. 2 lie on top of the wing of the laser line.)

The reason that the $n=1$ peak is smaller than the $n=2$ peak on the side of the light scattering spectrum where the surface mode appears can be easily seen in Fig. 6. It is simply a natural result of the mixing of bulk and surface waves which is reflected in the fact that the spectral density of the $n=1$ mode is particularly reduced on the side of the film where the surface spin wave is localized.

We now explore the influence of spin pinning on the relative intensities of the modes, bearing in mind that in the data of Malozemoff *et al.* I_{S_1}/I_{S_2} is less than unity while I_{A_1}/I_{A_2} is greater than unity. In Fig. 8, we show a spectrum calculated with $\lambda_> = \lambda_< = 5/L$, where L is the film thickness. This value for $\lambda_>$ and $\lambda_<$ corresponds to very strong pinning in the surface. If only spins in the very outermost surface layer are subject to the pinning field, and the strength of the pinning field H_s is given by the expression $2D\lambda/a_0$ quoted earlier, then $H_s \cong 5\times10^4$ Oe for $a_0=3$ Å. A pinning field of this magnitude is unlikely to be in-

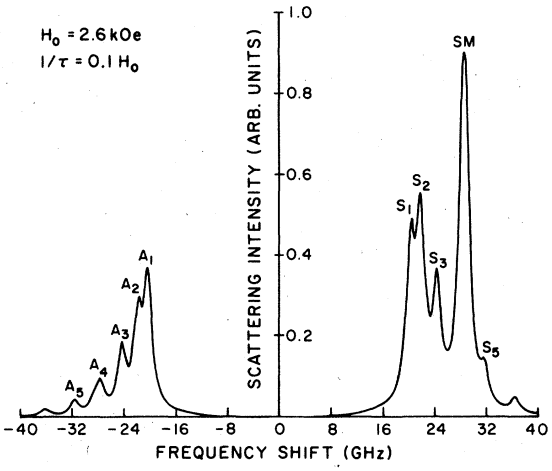

FIG. 7. Brillouin spectrum for a 1060-Å-thick film of $Fe_{80}B_{20}$. The scattering geometry is that used in the experiments of Grimsditch *et al.* (Ref. 2) where the incident photon of wavelength 5145 Å is polarized in the xy plane and the angle $\theta_0=59°$ while $\theta_s=0°$. Other parameters relevant to the sample are $4\pi M_s=15$ kOe and $D=1.4\times10^{-9}$ Oe cm^2. The Damon-Eshbach surface wave peak is labeled by SM and S_1–S_5 and A_1–A_5 denote the Stokes and anti-Stokes bulk standing modes, respectively.

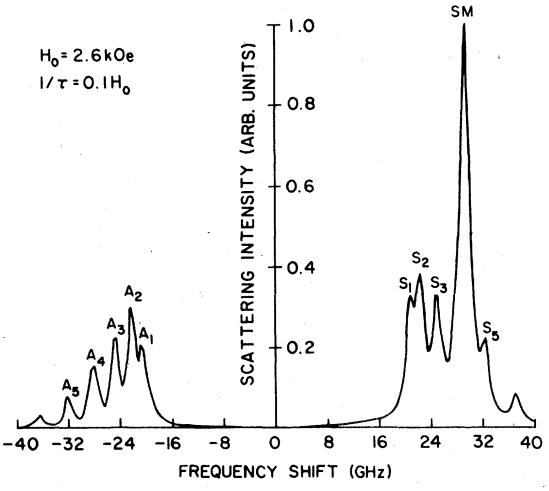

FIG. 8. Effect of surface pinning on the Brillouin spectrum for the sample and the setup identical to that in Fig. 7. The pinning parameters $\lambda_<$ and $\lambda_>$ for the upper and lower surface, respectively, are both taken to be $5/L$, where $L=1060$ Å.

trinsic in origin, but may be generated by an oxide layer on the surface. This strong pinning field at both the surfaces seems to affect the modes S_1, S_2, and A_1 most dramatically. In each case the intensity of the mode is reduced from that in the absence of pinning on the surfaces. Thus while the intensity ratio I_{S_1}/I_{S_2} is changed only slightly (to a value closer to unity), the ratio I_{A_1}/I_{A_2} is drastically reduced to a value less than unity. On both accounts, the spectrum in Fig. 8 looks less like the data than that in Fig. 7.

In Fig. 9, the pinning parameter on the surface $y=0$ equals $5/L$, while we have no pinning on the surface at $y=L$. The ratio I_{S_1}/I_{S_2} is now reduced well below unity, but the ratio I_{A_1}/I_{A_2} also remains well below unity.

The characteristics of the spectrum in Fig. 7, and most particularly the behavior of the ratios I_{A_1}/I_{A_2} and I_{S_1}/I_{S_2} suggest to us that in the films studied by Malozemoff *et al.*, the spins in the surfaces are not subject to strong pinning fields.

We can see that there is a very great difference between the ratio I_{S_1}/I_{S_2} and also I_{A_1}/I_{A_2} when a pinning field is imposed on the upper surface only, and when it is imposed on only the lower surface. This is illustrated in Fig. 10, where we present a spectrum for the choice $\lambda_<=0$ and $\lambda_>=5/L$. Here we find that the ratios I_{S_1}/I_{S_2} and I_{A_1}/I_{A_2} become greater than unity.

The trends in the above figures can be understood by recalling from ferromagnetic resonance theory[18] that when spin pinning is present on the boundary,

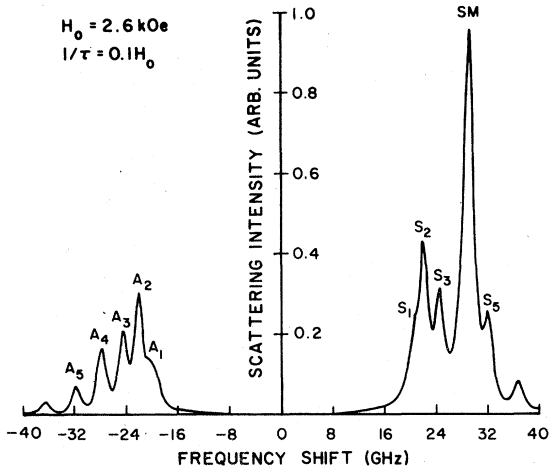

FIG. 9. Here we introduce a strong pinning field on only the upper surface such that $\lambda_<=5/L$ and $\lambda_>=0$. All other parameters are same as in Fig. 7.

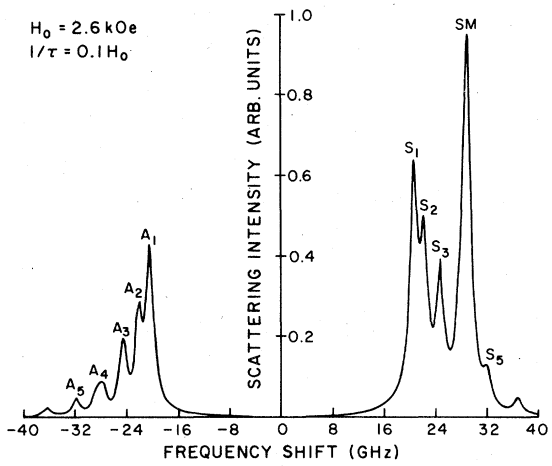

FIG. 10. This is the Brillouin spectrum for the $Fe_{80}B_{20}$ film when the top surface is unpinned and the bottom surface is strongly pinned. Here $\lambda_<=0$ and $\lambda_>=5/L$ and all other details are the same as that in Fig. 7.

the eigenfunctions of the lowest-lying modes are affected most strongly. To see this, consider a scalar wave $\psi(y)$ on the half space $0\leq y\leq\infty$, and suppose the wave is subjected to a boundary condition similar in form to those used in our spin-wave theory:

$$\frac{d\psi}{dy}+\lambda\psi=0 \quad . \tag{4.2}$$

If we seek a solution of Eq. (4.2) of the form $\psi(y)=\sin(k_\perp y+\phi)$, then ϕ is determined from the condition

$$\cot\phi=\frac{\lambda}{k_\perp} \quad . \tag{4.3}$$

Thus, as $k_\perp\to 0$, $\phi\to 0$, and $\psi(y)=\sin(k_\perp y)$ corresponding to a "completely pinned" solution. If $k_\perp >> \lambda$, then $\phi\cong\frac{1}{2}\pi$, and the solution is an "unpinned" wave with $\psi(y)=\cos(k_\perp y)$.

Hence, if we compare Fig. 7 with Fig. 9, we see the addition of pinning to the surface $y=0$ not only decreases the intensity of the whole spectrum, but decreases I_{S_1} by an amount greater than I_{S_2}, so (I_{S_1}/I_{S_2}) is lowered and so also (I_{A_1}/I_{A_2}). The intensity ratios of the higher modes are much less affected, so it is these particular intensity ratios that are most sensitive to the presence of pinning.

In Fig. 10, we see (I_{S_1}/I_{S_2}) and (I_{A_1}/I_{A_2}) are *increased* by the addition of pinning on the back surface $y=L$. This may be understood by resorting again to the example of a simple scalar wave $\psi(y)$ confined to a film $0\leq y\leq L$. If unpinned boundary conditions are applied to each surface, the normalized lowest eigenfunction is simply the constant $\psi_0(y)=L^{-1/2}$.

While for strong pinning at the surface $y = L$ [so $\psi(y)$ must vanish there] and no pinning on the surface $y = 0$, the normalized lowest eigenfunction is $\tilde{\psi}_0(y) = (2/L)^{1/2}\cos(\pi y/2L)$. Notice that as $|\tilde{\psi}_0(0)/\tilde{\psi}_0|^2 = 2$, pinning on the *back* surface enhances the amplitude of the lowest eigenmode near the front surface which is exposed to the light. The effect is less dramatic for the next highest eigenmode and, as shown in Fig. 9, the ratio (I_{S_1}/I_{S_2}) becomes greater than unity.

We see the intensity ratios (I_{S_1}/I_{S_2}) and (I_{A_1}/I_{A_2}) can tell us a great deal about the nature of the pinning present at the film surface. The fact that the skin depth δ is small compared to L, so the region near only *one* surface is illuminated, allows us to tell *which* surface is subjected to strong pinning, if we have $\lambda_< \neq \lambda_>$. Note that in microwave resonance studies, where the microwave skin depth δ is large compared to L for such thin films, the intensity ratios for the case $\lambda_> = 5/L$ and $\lambda_< = 0$ will necessarily be the same as that for $\lambda_> = 0$ and $\lambda_< = 5/L$ and it is not possible to distinguish between the pinning at the two interfaces.

In the ferromagnetic resonance studies on epitaxially grown YIG films carried out by Wigen and coworkers,[18] when the Zeeman field was parallel to the film surfaces, the spins on one surface experienced effective pinning fields antiparallel to the applied Zeeman field. In this circumstance, a surface spin wave is driven out of the bulk spin-wave manifold, to appear at a frequency *below* $\gamma(H_0B)^{1/2}$. These waves, described by Wigen *et al.* as exchange surface waves, have a character fundamentally different from the Damon-Eshbach wave. The Damon-Eshbach wave exists as a long lived spin wave only for wavelengths sufficiently long that the Zeeman and dipolar energies dominate its excitation energy, while exchange energy is negligible. In fact, in the presence of exchange, the wave is not a true elementary excitation of the semi-infinite system, but acquires a finite lifetime by radiating its energy into the bulk of the material in the form of bulk spin waves.[7] In contrast to this, the surface spin waves explored in Ref. 18 exist as well-defined elementary excitations if only exchange is present; of course in practice, dipolar coupling between the spins affects the properties of these modes importantly, but in contrast to the Damon-Eshbach wave, these modes exist even if dipole interactions are absent.

In Fig. 11 we show the light scattering spectrum for the case where the surface pinning field at $y = 0$ is antiparallel to the Zeeman field ($\lambda_< = -5/L$ and $\lambda_> = 0$). For comparison we have included the spectrum of Fig. 9 with $\lambda_< = +5/L$ and $\lambda_> = 0$ (i.e., parallel pinning field on top surface only), in this figure. We see prominent lines produced by scattering from the exchange dominated surface spin waves

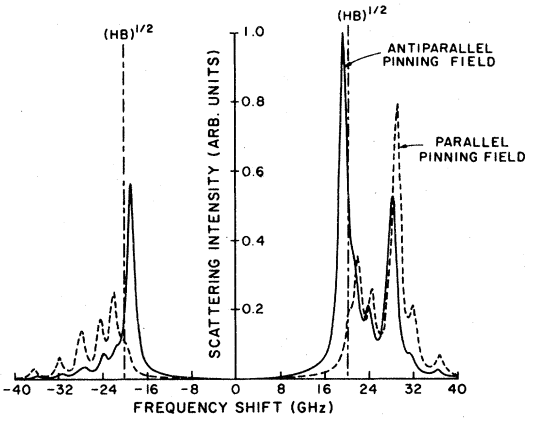

FIG. 11. Comparison of the effect on the Brillouin spectrum of a strong pinning field (at the upper surface) which is antiparallel to the Zeeman field with one that is parallel to it. The sample and setup is the same as in the previous figures. For the solid curve $\lambda_< = -5/L$ and $\lambda_> = 0$ while for the dashed curve, as in Fig. 9, $\lambda_< = 5/L$ and $\lambda_> = 0$.

very similar in character to those observed in the ferromagnetic resonance studies. These are the features which lie *below* the frequency $\gamma(H_0B)^{1/2}$, the lowest possible bulk spin-wave frequency for the present geometry, where the wave vector of the spin wave lies in the plane perpendicular to the bulk magnetization. It should be noted that in the light scattering spectrum, under the condition that the skin depth is small, the exchange surface spin waves are intense features in the spectrum while in the microwave resonance work, they are very weak compared to the uniform mode, since the field extends throughout the sample. There is a surface spin-wave feature on both the Stokes and the anti-Stokes side of the line, indicating that the exchange dominated surface spin waves can propagate in both directions across the magnetization. In fact, in the absence of dipole coupling between the spins, "exchange only" surface spin waves display none of the dramatic nonreciprocal properties we see in the Damon-Eshbach waves. Note the pronounced Stokes–anti-Stokes asymmetry present in the exchange surface spin-wave intensity ratio. The presence of this asymmetry attests to the quantitative influence of dipolar coupling between the spins on the properties of the mode. The intensity ratio would be unity [if the very small correction produced by $\exp(\hbar\Omega/k_BT)$ is overlooked] in the presence of only exchange coupling between the spins.

In Fig. 12, for the case where both the incident and scattered photon lie in the xy plane, we plot a number of spectra which display the manner in which the bulk spin-wave Stokes–to–anti-Stokes ratio depends on the scattering geometry. We have fixed the angle of incidence θ_0 to be equal to 60°, the in-

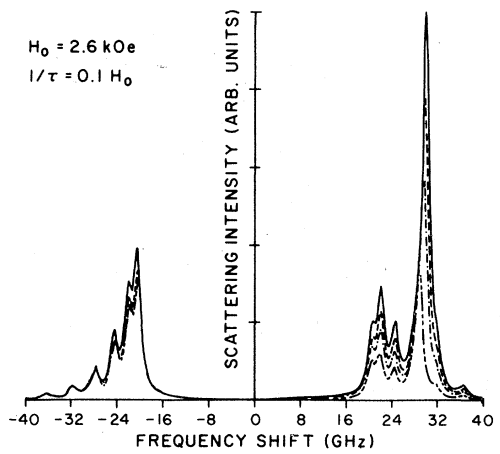

FIG. 12. Incident angle for these spectra is fixed at 60° while the scattering angle is varied from 0 to 60°. The film is again of $Fe_{80}B_{20}$ with $L = 1060$ Å, $4\pi M_s = 15$ kOe, and the exchange constant $D = 1.4 \times 10^{-9}$ Oe cm^2. The incident light of wavelength 5145 Å is polarized along the $\hat{z}$ direction. The solid curve is for back scattering, i.e., $\theta_s = 60°$, the $(--)$ curve has $\theta_s = 45°$, the $(-)$ curve has $\theta_s = 30°$, and finally $\theta_s = 0°$ for the $(---)$ curve.

cident light is polarized along the $\hat{z}$ direction and several spectra for various values of θ_s are super imposed. When $\theta_s = \theta_0$, which is the geometry employed by Sandercock in his study of very thick films, the Stokes–anti-Stokes asymmetry is rather small, as in Fig. 3 where the differences are quite subtle. However, as the scattered photon direction is moved up toward the normal to the film, the Stokes–anti-Stokes asymmetry becomes more and more pronounced.

Up to this point, we have presented results where the propagation direction of the magnon was perpendicular to the applied field, i.e., $\phi_s = 0$ in Fig. 2. The case where the magnon propagation is at some angle with respect to the field is also quite interesting. In the absence of exchange, Damon and Eshbach predicted that the surface spin wave would propagate only for a restricted set of directions.[30] In particular, on the top surface the surface mode would exist for a cone of angles, $-\phi_c \leq \phi_s \leq \phi_c$, where ϕ_s (as in Fig. 2) is the angle between the x axis and $Q_{\parallel}$ and ϕ_c is given by the equation $\cos\phi_c = (H/B)^{1/2}$. On the bottom surface the surface mode is allowed for a cone of angles directed in the opposite direction $\pi - \phi_c \leq \phi_s \leq \pi + \phi_c$. At the critical angle ϕ_c the frequency of the surface wave intersects the bulk spin-wave band.

The angular dependence of the properties of the surface spin wave in the presence of exchange, in thin films, has not been extensively discussed.[1,7,31] In a semi-infinite material, in the presence of exchange, there are always some bulk spin waves at the same frequency as the surface spin wave. As a result, the surface wave mixes with the bulk waves and acquires a "leaky" character in that it loses energy to the bulk waves. This was originally pointed out by Wolfram and de Wames[1] for propagation perpendicular to the field. It has been shown[7] that as the critical angle is approached the surface mode mixes more strongly with the bulk modes and becomes less localized near the surfaces. As we shall see below, there is a similar behavior in thin films except that the concept of a distinct critical angle loses much of its meaning.

In Fig. 13 we present dispersion relations for the bulk and surface modes for various angles of propagation. The parameters here and in the remainder of the paper are the same as those used for Fig. 5 for a thin Fe film. The dispersion curves show the dependence of the frequency of the peaks of different modes of the spectral density function on the magnitude of the wave vector $\vec{Q}_{\parallel}$. We see that as the wavelength of the surface mode becomes large com-

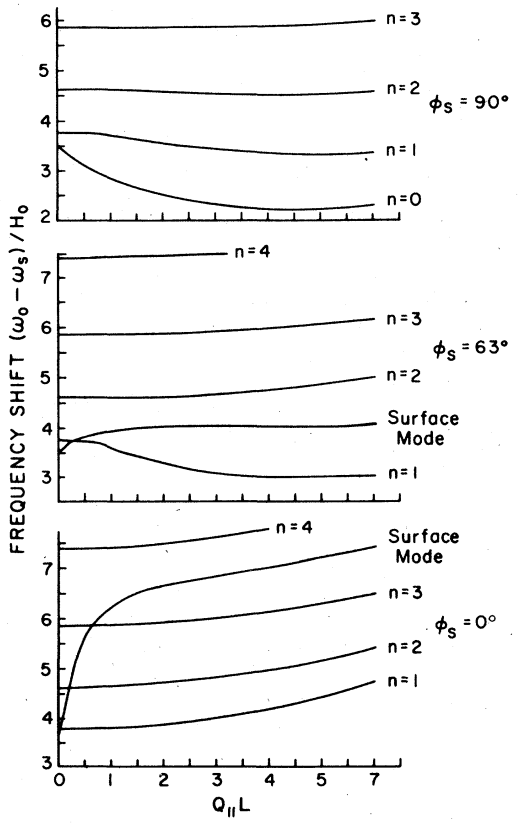

FIG. 13. Dispersion relations for an 880-Å Fe film for several angles of propagation. Here ϕ_s denotes the angle between the propagation wave vector $Q_{\parallel}$ and the x axis.

pared to the thickness of the sample ($Q_{\parallel}L \to 0$), the frequency of the surface wave drops. Eventually the surface mode lies underneath all the allowed bulk modes. As ϕ_s increases, this crossing occurs at larger values of $Q_{\parallel}L$. For propagation parallel to the field there is no surface mode. The surface mode has been replaced by the $n=0$ mode.

In Fig. 14 we present a typical light scattering spectrum for a 880-Å-thick film of Fe as a function of the angle ϕ_s. The geometry for this figure is $\theta_0 = \theta_s = 45°$. As expected from the Damon and Eshbach results and the dispersion relations above, we see that as ϕ_s is increased, the surface wave peak moves down in frequency. Also as the Damon-Eshbach critical angle is approached ($\phi_c = 73.5°$), we see that the intensity of the surface peak on the Stokes side is reduced. On the anti-Stokes side there is no surface peak for propagation at $\phi_s = 0$, but as ϕ_s increases scattering from the surface wave localized on the bottom surface starts to appear. We may understand this in the following way. At $\phi_s = 0$, the surface waves on the top and bottom are well localized. Thus on the Stokes side we can create a surface wave at the top, but we cannot destroy a surface wave at the bottom on the anti-Stokes side because the light does not penetrate far enough. As the critical angle is approached, the surface waves take on more bulk character and are not as well localized. Thus for propagation near the critical angle, the light "sees" the spectral density of both the surface spin wave at the top and the one at the bottom. As a result one sees peaks from scattering from surface spin waves on both the Stokes and anti-Stokes sides.

The above argument is illustrated by Fig. 15. Here we plot the spectral density versus depth for the surface spin-wave mode peaks seen in Fig. 14. As before, this gives us the square of the eigenvector of the mode. Peaks on the Stokes side of Fig. 14 represent a sampling of the $y=0$ side of Fig. 15, and peaks on the anti-Stokes sides represent a sampling of the $y=L$ side of Fig. 15. This is because, in the absence of inequivalent pinning conditions, reversing the frequency is equivalent to turning the crystal upside down, i.e., $S_{xx}(\Omega, y=0) = S_{xx}(-\Omega, y=L)$. Essentially what we see in Fig. 15 is that as ϕ_s increases the surface mode becomes less localized in that the strength on the $y=L$ side nears that of the $y=0$ side. As the critical angle is approached, the surface mode merges into the $n=1$ mode and the $n=1$ mode merges into the $n=0$ mode. We see also in Fig. 15 that there is no distinct critical angle. For example, well below the Damon-Eshbach critical angle of 73.5° we see that the surface mode is already less localized.

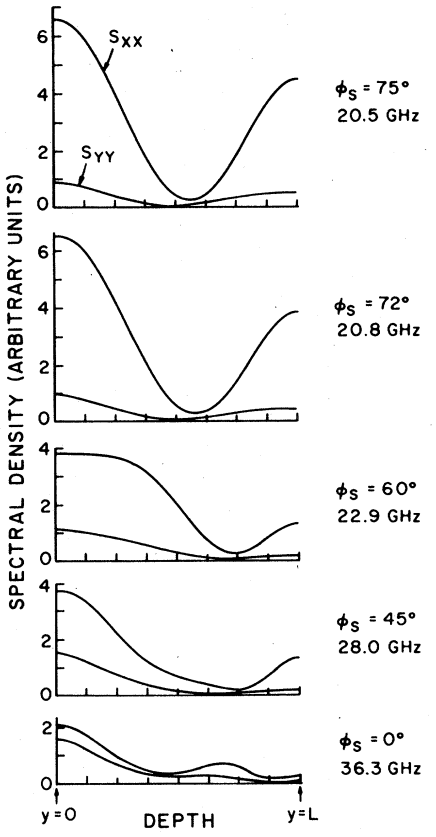

FIG. 15. Spectral density vs depth for the surface spin-wave peaks seen in Fig. 14. As ϕ_s increases the spectral density on the $y=L$ side nears the value on the $y=0$ side.

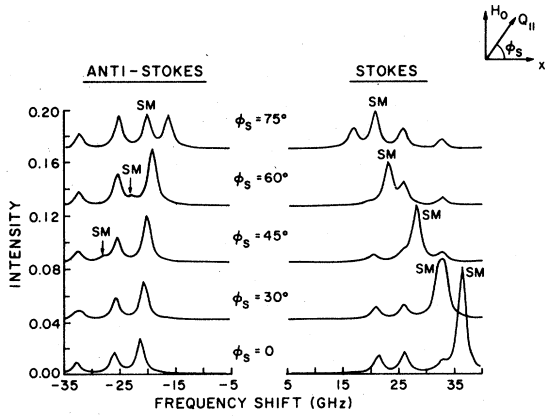

FIG. 14. Light scattering spectrum from an 880-Å Fe film as a function of the propagation angle. Note as ϕ_s increases, one sees scattering from surface spin waves on both sides of the spectrum.

In this paper, we have presented the theory of light scattering from spin waves in thin ferromagnetic films. We have discussed a number of general features of the spectra, and illustrated these with numerical calculations carried out for parameters ap-

propriate to films formed from ferromagnetic metals. Our calculated spectra seem in very good accord with the data reported by Grimsditch and co-workers, so the theory appears to be sufficiently reliable that the nature of surface pinning in these samples can be extracted by fits to the measured mode intensities. We feel that the light scattering method should prove a powerful addition to the experimental methods used in magnetism, and hope to see more laboratories engaged in such measurements in the future.

ACKNOWLEDGMENTS

The research of two of us (T.S.R. and D.L.M.) was supported by the Air Force Office of Scientific Research, under Contract No. F49620-78-C-0019.

[1]T. Wolfram and R. E. de Wames, Prog. Surf. Sci. 2, 233 (1972).

[2]M. Grimsditch, A. Malozemoff, and A. Brunsch, Phys. Rev. Lett. 43, 711 (1979).

[3]P. Grünberg and F. Metawe, Phys. Rev. Lett. 39, 1561 (1977); J. R. Sandercock and W. Wettling, IEEE Trans. Magn. 14, 442 (1978); J. Appl. Phys. 50, 7784 (1979).

[4]A general discussion of light scattering under these circumstances, with emphasis on the influence of the surface on the spectrum has been given by D. L. Mills and K. R. Subbaswamy, Prog. Opt. (in press).

[5]It should be remarked that the theory has been developed independently at Stuttgart and Irvine, and we have joined together to produce a single general discussion of the material.

[6]R. E. Camley and M. Grimsditch, Phys. Rev. B (in press).

[7]R. E. Camley and D. L. Mills, Phys. Rev. B 18, 4821 (1978); Solid State Commun. 28, 321 (1978).

[8]M. G. Cottam J. Phys. C 12, 1709 (1979).

[9]C. Kittel, Phys. Rev. 110, 1295 (1958).

[10]G. Rado, Phys. Rev. B 18, 6160 (1978).

[11]See, for example, the coupling mechanism described in Eq. (4.1) of Ref. 7.

[12]M. Sparks, Phys. Rev. B 1, 3831, 3856, 3869 (1970).

[13]T. Wolfram and R. E. de Wames, Phys. Rev. B 4, 3125 (1971).

[14]R. Henry, S. D. Brown, P. E. Wigen, and P. J. Besser, Phys. Rev. Lett. 28, 1272 (1972).

[15]R. E. Camley, Phys. Lett. 45, 283 (1980).

[16]See C. Kittel, *Quantum Theory of Solids* (Wiley, New York, 1963), Chap. 4.

[17]See the chapter on the electromagnetic field in A. A. Abrikosov, L. P. Gorkov, and I. E. Dzyaloshinski *Methods of Quantum Field Theory in Statistical Mechanics* (Prentice-Hall, Englewood Cliffs, N. J., 1963). Here it is demonstrated that the retarded Green's functions formed from the field operators in quantized electrodynamics obey the same differential equation and boundary conditions as their classical counterparts. Hence, both sets of functions are identical, and the results of the classical analysis and the quantum field theory must agree.

[18]J. T. Yu, R. A. Turk, and P. E. Wigen, Phys. Rev. B 11, 420 (1975).

[19]I. Harada, O. Nagai, and T. Nagamiya, Phys. Rev. B 16, 4882 (1977).

[20]See L. D. Landau and E. M. Lifshitz, *Electrodynamics of Continuous Media* (Pergammon, Oxford, 1960), p. 331.

[21]H. Le Gall, Tran Khanh Vien, and B. Desormiere, Phys. Status Solidi 47, 591 (1971). We were unaware of this paper at the time our earlier work was completed, and as a consequence it was not cited in Ref. 7. We are most grateful to Dr. Le Gall for sending us a reprint of it.

[22]W. Wettling, M. G. Cottam, and J. R. Sandercock, J. Phys. C 8, 211 (1975).

[23]Some care must be exercised when the Stokes–to–anti-Stokes ratio is discussed. In this paragraph, and elsewhere in the present paper we consider the spectrum associated with the light scattered into a given final *direction* and in the scattering of an incident photon of wave vector $\vec{k}_0$ to a photon of wave vector $\vec{k}_s$ we associate the Stokes process with that in which a spin wave of wave vector $\vec{Q}$ is created and the anti-Stokes process with that where a spin wave of wave vector $-\vec{Q}$ is absorbed. In the presence of time-reversal symmetry the later process (anti-Stokes) is equivalent to the scattering from $-\vec{k}_s$ to $-\vec{k}_0$ with the absorption of spin wave of $+\vec{Q}$. In this event, the Stokes–to–anti-Stokes intensity ratio, from the principle of detailed balance is $\exp(\hbar\Omega/kT)$. A careful discussion of the connection between time-reversal symmetry and the Stokes–to–anti-Stokes ratio has been given by R. Loudon, J. Raman Spectros. 7, 10 (1978).

[24]J. Sandercock, J. Appl. Phys. 50, 7784 (1979).

[25]A discussion of these waves, and references to earlier theoretical analyses, has been given by R. E. Camley, J. Appl. Phys. 50, 5272 (1979).

[26]See J. J. Brion, R. F. Wallis, A. Hartstein, and E. Burstein, Phys. Rev. Lett. 28, 1455 (1972).

[27]Bernardo Laks and D. L. Mills, Phys. Rev. B (in press).

[28]See, for example, D. L. Mills, Y. J. Chen, and E. Burstein, Phys. Rev. B 13, 4419 (1976).

[29]In the finite film, and in the presence of exchange, all the eigenmodes have complex character and are in fact a linear superposition of waves made up from each of the six attenuation constants κ_i. For the parameters considered here, the dominant term in the eigenfunctions of the surface mode localized on the upper surface is an exponential which decays to zero as one moves into the film from the upper surface. Similarly, for the surface spin-wave mode on the lower surface the eigenfunction receives its dominant contribution from a decaying exponential localized on the surface $y = L$. In the review article by Wolfram and de Wames (Ref. 1) the properties of normal modes in the ferromagnetic film are discussed in detail.

[30]R. W. Damon and J. R. Eshbach, J. Phys. Chem. Solids 19, 308 (1960).

[31]P. Hansen and U. Krey, Z. Angew Phys. 32, 104 (1971).